ORIGIN OF LATE PLEISTOCENE BRYOZOAN REEF MOUNDS; GREAT AUSTRALIAN BIGHT

NOEL P. JAMES,[1] DAVID A. FEARY,[2*] CHRISTIAN BETZLER,[3] YVONNE BONE,[4] ANN E. HOLBOURN,[5] QIANYU LI,[4] HIDEAKI MACHIYAMA,[6] J.A. TONI SIMO,[7] AND FINN SURLYK[8]

[1] *Queen's University, Kingston, Ontario K7L 3N6, Canada*
e-mail: james@geol.queensu.ca
[2] *Geoscience Australia, Canberra ACT 2601, Australia*
[3] *Hamburg University, 20146 Hamburg, Germany*
[4] *Adelaide University, Adelaide South Australia 5005, Australia*
[5] *Christian-Albrechts, University, Kiel D-24118, Germany*
[6] *Japan Marine Science and Technology Center, Kanagawa 237-0061, Japan*
[7] *University of Wisconsin, Madison, Wisconsin 53706, U.S.A.*
[8] *University of Copenhagen, 1350 Copenhagen K, Denmark*

ABSTRACT: **Bryozoan-rich biogenic mounds grew periodically on the prograding carbonate slope of the central Great Australian Bight throughout Pliocene–Pleistocene time. Cores from three ODP Leg 182 drill sites provide a record of mound growth during the last 300,000 years over a stratigraphic thickness of ~ 150 m. These mounds, the first such structures described from the modern ocean, grew between paleodepths of 100 and 240 m; we infer that the upper limit of growth was established by swell wave base, and the lower boundary was fixed by an oligotrophic water mass. Detailed chronostratigraphy, based on radiometric and U-series dating, benthic foraminifer stable-isotope stratigraphy, and planktonic foraminifer abundance ratios, confirms that buildups flourished during glacial lowstands (even-numbered marine isotope stages) but were largely moribund during interglacial highstands and are not extant today.**

Mound floatstones are compositionally a mixture of *in situ* bryozoans comprising 96 genera and characterized by fenestrate, flat robust branching, encrusting, nodular–arborescent, and delicate branching growth forms. The packstone matrix comprises autochthonous and allochthonous sand-size bryozoans, benthic and planktonic foraminifers, serpulids, coralline algae, sponge spicules, peloids, and variable glauconite and quartz grains, together with mud-size ostracods, tunicate spicules, bioeroded sponge chips, and coccoliths. Intermound, allochthonous packstone and local grainstone contain similar particles, but they are conspicuously worn, abraded, blackened, and bioeroded.

An integrated model of mound accretion during sea-level lowstands begins with delicate branching bryozoan floatstone that increases in bryozoan abundance and diversity upward over a thickness of 5–10 m, culminating in thin intervals of grainstone characterized by reduced diversity and locally abraded fossils. Mound accumulation was relatively rapid (30–67 cm/ky) and locally punctuated by rudstones and firmgrounds. Intermound highstand deposition was comparatively slow (17–25 cm/ky) and typified by meter-scale, fining-upward packages of packstone and grainstone or burrowed packstone, with local firmgrounds overlain by characteristically abraded particles.

Mound growth during glacial periods is interpreted to have resulted from increased nutrient supply and enhanced primary productivity. Such elevated trophic resources were both regional and local, and thought to be focused in this area by cessation of Leeuwin Current flow, together with northward movement of the subtropical convergence and related dynamic mixing.

INTRODUCTION

Ocean Drilling Program (ODP) Leg 182 in the Great Australian Bight (Feary et al. 2000) cored upper Pleistocene bryozoan mounds and associated cool-water carbonate sediments at three of eight shelf-edge and uppermost slope locations, Sites 1129, 1131, and 1132 (Fig. 1). These are the first such buildups cored in a Quaternary continental-margin setting. Interim results were briefly reported by James et al. (2000), Holbourn et al. (2002), and Bone and James (2002). This paper documents these biogenic structures more thoroughly, with particular emphasis on their temporal, sedimentological, and paleontological attributes. Similar bryozoan biogenic mounds are a recurring phenomenon throughout the Phanerozoic, and their origin is one of the most controversial topics in carbonate sedimentology (Tucker and Wright 1990; James and Bourque 1992; Monty et al. 1995). This study, focused on the relationship between oceanography and mound growth, provides new insights into how these contentious structures can be interpreted in the geological record.

The Great Australian Bight (GAB) has an unusually broad (up to 200-km-wide) continental shelf (Fig. 1) that is covered by cool-water carbonate sediment (Wass et al. 1970; James and von der Borch 1991; James et al. 1994; James et al. 2001). Predominately coarse-grained shelf sediment grades seaward into fine-grained sandy and muddy carbonate at and beyond the shelf edge, below water depths of ~ 200 m (James et al. 2001). The upper slope in the central and western GAB is a thick, southward-prograding wedge of Neogene sediment (Fig. 2) that downlaps onto and forms part of the Eyre Terrace (James and von der Borch 1991; Feary and James 1998; Feary et al. 2000) such that the margin resembles a distally steepened ramp (cf. Read 1985). The mounds described here occur immediately seaward of the shelf edge at the transition between shelf and slope environments in a ''mid-ramp'' setting. They were cored at three sites, two immediately seaward of the shelf edge (at 203 and 218 m water depth) and one downslope (in 334 m water depth) (Figs. 1, 2).

METHODOLOGY

Seismic

Regional seismic stratigraphy for the Cenozoic succession of the central and western Great Australian Bight was established on the basis of detailed seismic stratigraphic analysis and interpretation of a grid of 2,350 km of high-quality, regional 2-D seismic reflection lines collected over an area of 155,000 km^2 on the continental shelf and upper slope (Feary and James 1998). The mound morphology visible on these seismic lines (Feary and James 1995) prompted the collection of an additional 1800 line-km of 2-D seismic data as 0.5 nautical-mile spaced grids centered on prospective drill sites, together with tielines between sites. These high-resolution data were collected with a 1000-m 80-channel analogue streamer, using a single array of three SSI-GI airguns in full bubble-suppression mode at 2000 psi and 3 m depth (Feary 1997). Data are 3.5 second records with a 12.5 m shot interval and a 1 millisecond sample rate.

* Present address: Academy of Sciences, Washington, D.C. 20418, U.S.A.

JOURNAL OF SEDIMENTARY RESEARCH, VOL. 74, NO. 1, JANUARY, 2004, P. 20–48
 1527-1404/04/074-20/$03.00

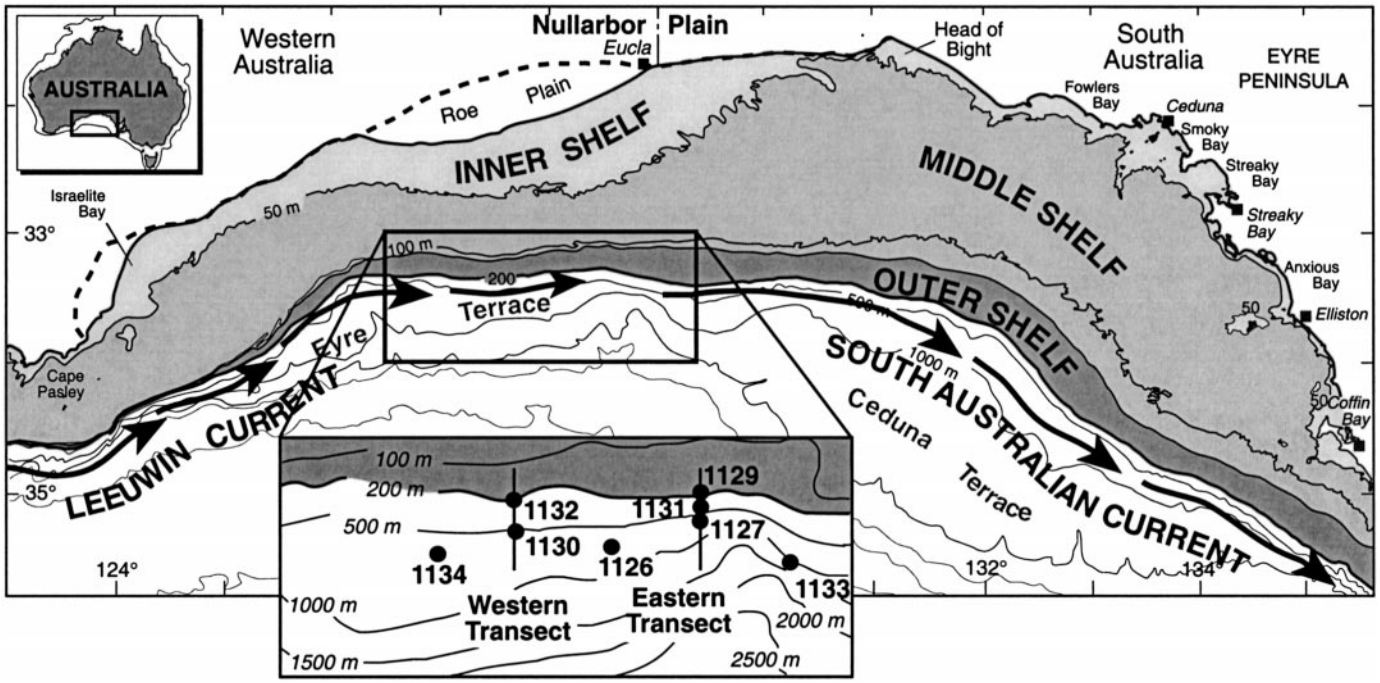

FIG. 1.—Location of study area (inset), bathymetry of Great Australian Bight, and location of ODP sites.

Laboratory

Coring and Sampling.—The succession was cored using standard ODP advanced piston core and extended core barrel techniques (Feary et al. 2000). Cores were split, logged, and sampled at sea. They were relogged in greater detail at the ODP core repository and many more samples were taken, of which 291 were used for this study. Each sample was ~ 75 cc, of which 15 cc were used for thin-section analysis and 60 cc for binocular analysis of bryozoans, foraminifers, and sediment (Tables 1, 2, 3). The 60 cc subsample was sieved into > 1000 μm (very coarse sand and coarser), 1000–63 μm (coarse to very fine sand), and < 63 μm mud size fractions, herein referred to as the coarse, sand, and mud fractions.

Most sediment is packstone or floatstone and was named using a modification of the Dunham (1962) and Embry and Klovan (1971) schemes. Sand and finer-grained sediment was described in the usual way except that, because most material is fine-grained packstone, these sediments were further subdivided into muddy packstone (> 50% mud matrix) and grainy packstone (< 50% mud matrix). Similarly, most coarse-grained sediment is floatstone with the sediment described as rich floatstone if it contained > ⅓ by volume > 2 mm particles, and termed a sparse floatstone if there was < ⅓ such biofragments. Most sediments contain a few floating bryozoan particles but were called floatstones only if such particles were large and conspicuous. Lithologic units (Fig. 3) were defined on the basis of major sediment types.

Fossils.—Bryozoans and foraminifers were identified under the binocular microscope and volumetric percentages estimated using standard comparison charts. Whereas most bryozoans could be readily identified (Appendix 1, see Acknowledgments), up to 25% in some samples could not be assigned to a genus, usually because of abrasion or cement infilling zooids. Zooids in packstone units, although abundant, are usually too fragmented to be identified.

Radioisotopic Dating.—Nodular–arborescent bryozoans and large benthic foraminifers were selected for isotopic age dating (Appendix 2, see Acknowledgments). Preparation methods are given in Holbourn et al. (2002) and Machiyama et al. (2003).

Samples were examined at all stages under a binocular microscope for any adhering cement and rejected if any was found. Mineralogy was determined by standard X-ray diffraction techniques. Samples were then analyzed by accelerator mass spectrometry for ^{14}C age at Isotrace Laboratory (University of Toronto) using techniques described by Litherland and Beukens (1995) and at the Leibniz Laboratory (Christian-Albrechts University, Kiel) using techniques described by Nadeau et al. (1997) and Schleicher et al. (1998). Results are not corrected for reservoir effect.

Deeper subsurface samples were analyzed for U/Th age at McMaster University using techniques described by Li et al. (1989). The only bryozoan with enough carbonate to be used for U-series dating was *Celleporaria* sp. There are clearly two species of the genera in these sediments, neither of which have been described. One is aragonite (species 1), and one is low-magnesium calcite (LMC) (species 2). Aragonite *Celleporaria* sp. 1 was only used if it contained > 95% aragonite. LMC *Celleporaria* sp. 2 contained 3–6 mole % $MgCO_3$, and again was used only if pure. There was no direct way, however, other than visual observation, to ascertain whether this latter form had undergone subsurface diagenesis. Stable-isotope analyses (n = 13) indicate no low carbon or oxygen values that would be indicative of subaerial or meteoric-water diagenesis, nor do the values co-vary when plotted against one another, suggesting that the values are original. Finally, because the skeletons of *Celleporaria* sp. 2 are LMC already, there is little potential drive for alteration by marine burial fluids.

Stable Oxygen Isotopes.—Well preserved specimens of the epifaunal benthic foraminifers *Cibicidoides subhaidingerii* and *Planulina wuellerstorfi* and of the infaunal foraminifer *Uvigerina peregrina* were selected and an average of 10 to 14 specimens of each were utilized for stable oxygen isotope analysis. Analyses were made with a Finnigan MAT 251 mass spectrometer at Kiel University. The instrument is coupled on line

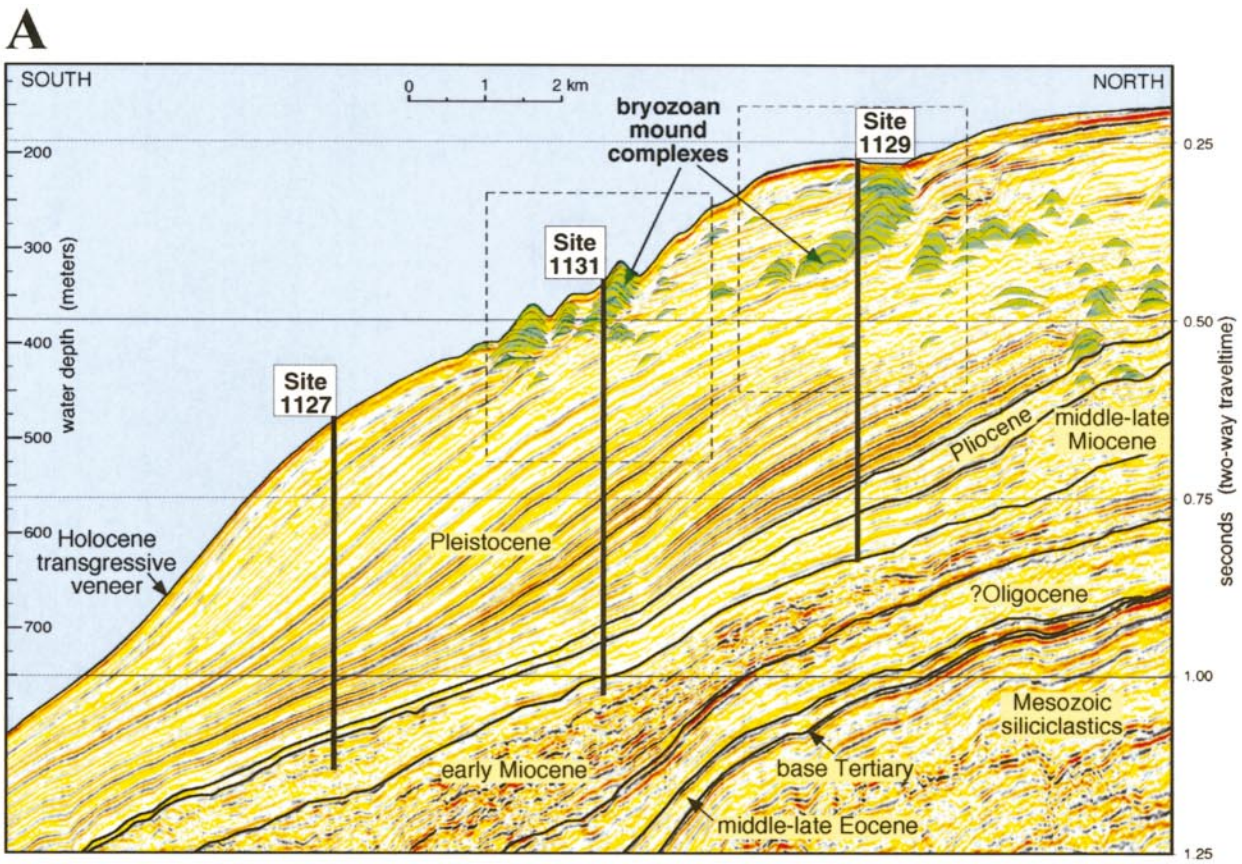
A
SOUTH
NORTH
0 1 2 km
bryozoan mound complexes
Site 1129
Site 1131
Site 1127
200
300
400
500
600
700
water depth (meters)
0.25
0.50
0.75
1.00
1.25
seconds (two-way traveltime)
Holocene transgressive veneer
Pleistocene
Pliocene
middle-late Miocene
?Oligocene
Mesozoic siliciclastics
early Miocene
base Tertiary
middle-late Eocene

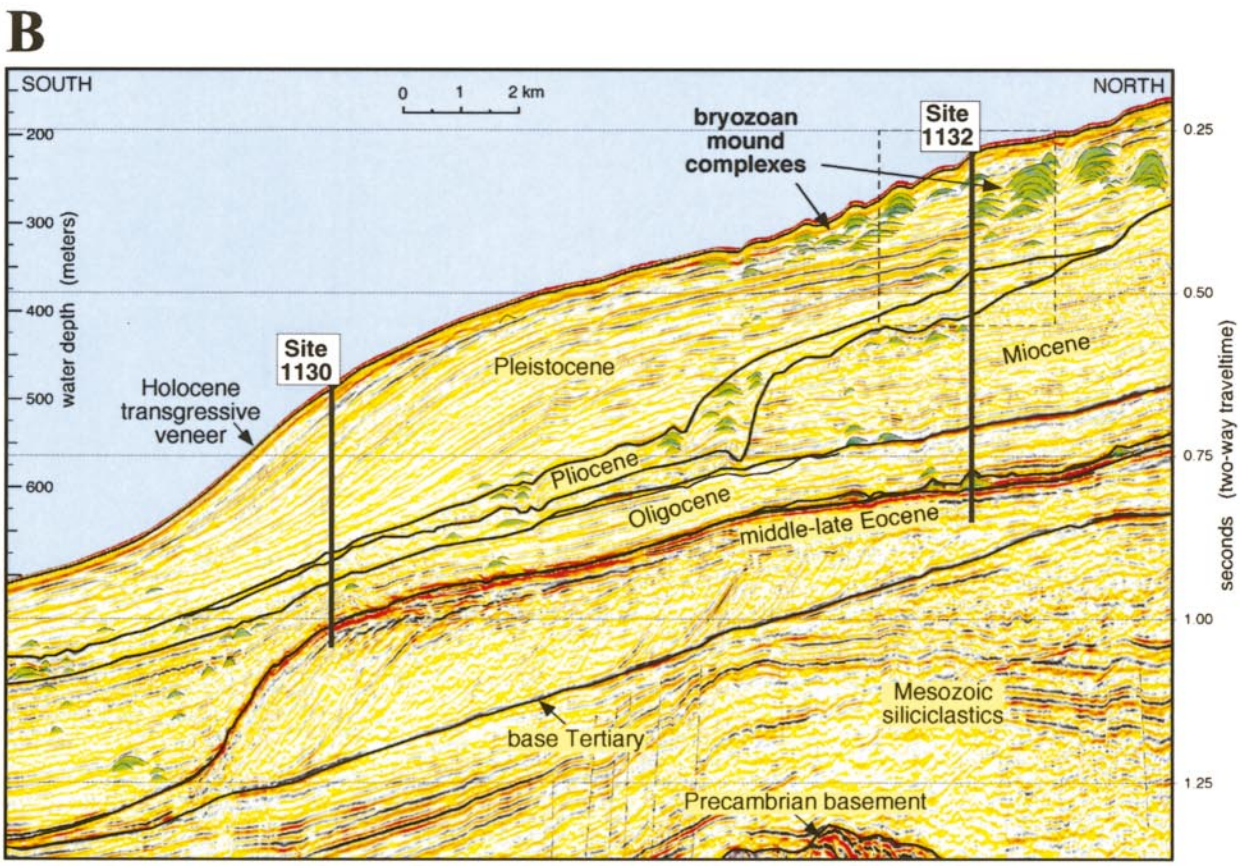
B
SOUTH
NORTH
0 1 2 km
bryozoan mound complexes
Site 1132
Site 1130
200
300
400
500
600
water depth (meters)
0.25
0.50
0.75
1.00
1.25
seconds (two-way traveltime)
Holocene transgressive veneer
Pleistocene
Miocene
Pliocene
Oligocene
middle-late Eocene
Mesozoic siliciclastics
base Tertiary
Precambrian basement

to a Carbo-Keil device for automated CO_2 preparation from carbonate samples for isotopic analysis. Samples were reacted by individual acid addition. The system has an accuracy (on the δ scale) of 0.05‰. The results were calibrated using the National Bureau of Standards and Technology (Gaithersburg, Maryland) carbonate isotope standard NBS 18, 19, and 20 and are reported on the Peedee Belemnite (PDB) scale (Holbourn et al. 2002).

RESULTS

Seismic Attributes

The broad, subdued-relief mounds within the Pleistocene succession are delineated by low- to moderate-amplitude reflections, representing slight to moderate impedance contrast between mound margins and surrounding sediment (Feary and James 1998). This contrasts with generally higher-amplitude, continuous or semicontinuous reflections in adjacent sediments. Seismic images show that the mounds are markedly elongate features, extending up to 10 km along slope and up to 750 m normal to the slope, with synoptic relief of up to $\sim$ 65 m. Four seismic facies are recognized: mound-core (convex-upward reflectors); mound-flank (concave downward reflectors); inter-mound (subparallel reflectors on and between mounds); and peri-mound (parallel reflectors occurring downslope from the mounds). Intermound facies are poorly delineated on seismic because of the relatively coarse resolution but are discernible in cores.

The subsurface disposition of mound structures is illustrated in two north–south sections, here called the eastern and western transects (Figs. 1, 2). These and other north–south sections across the western and central GAB margin (Feary and James 1998) show that the mounded reflectors are consistently present throughout the Pliocene–Pleistocene part of the prograding wedge underlying the modern outer shelf and upper slope. Although isolated mounds are located elsewhere in the succession, prolific mound growth leading to the development of the stacked mound complexes occurred in the same geomorphic position, immediately seaward of the shelf edge, throughout this period. Like the Plio-Pleistocene sediment wedge itself, the mound structures prograded 8–10 km through several hundred meters of section over the last 15 million years, with the most prolific mound growth occurring in the last 2 million years.

Eastern Transect.—Overall, Site 1129 is drilled through peri-mound, inter-mound, or mound-flank seismic facies (Fig. 4). The upper part of unit 2 is mound-core facies but most is peri-mound sediment seaward of large aggradational to retrogradational mounds some 0.5–1.0 km upslope. Unit 3 is either mound-core or mound-flank seismic facies, and unit 4 is peri-mound facies with mounds $\sim$ 0.5 km upslope. Unit 5 lies in peri-mound seismic facies.

Site 1131, downslope, at the distal, seaward end of this succession (Fig. 2), is drilled through a series of unit 2 mounds, with units 3 to 5 represented by well bedded peri-mound seismic facies (Fig. 5). The mounds illustrate an accretionary to retrogradational mode.

Western Transect.—Site 1132, the only one to intersect mounds on the western transect, cored mound-flank to mound-core lithologies (Fig. 6) of units 2 and 3. Strong reflectors of well-bedded peri-mound sediment characterize units 4 and 5.

Chronostratigraphy (Fig. 3).

Both radiocarbon and U-series dating are integrated with isotope stratigraphy and planktonic foraminifer abundance ratios to correlate the section with standard marine isotope stages (Figs. 3, 7, 8).

Radiocarbon Dating.—Analyses were performed mainly on the bryozoans *Celleporaria* and benthic foraminifers *C. subhaidingerii*) (Appendix 2, see Acknowledgments). The ^{14}C ages indicate that the top of unit 2 is 25,000 years old, the base of unit 2 is $>$ 50,000 years old, and the usefulness of ^{14}C age dates is limited to $\sim$ 15 to 20 mbsf (i.e., upper half of unit 2; Fig. 3). Analyses of bryozoans and foraminifers separated by a meter or less, for which there are four pairs, indicate close age correspondence. In two instances, there is a slight inversion of age from bryozoan samples in close proximity, possibly the result of burrowing.

U-Series Dating.—The U-series dates (Fig. 3; Appendix 2, see Acknowledgments) indicate an age of $\sim$ 11,000 ka for the top of unit 2 and ages $<$ 50,000 ka for the upper half of unit 2. The U-series dates also indicate that unit 3 is dominantly 120,000 to 290,000 years old (Fig. 3). Units 4 and 5 were not dated because the sediments are too old for the technique.

The ages derived by U-series dating are consistently younger than those acquired by ^{14}C dating of closely positioned samples (Fig. 3). This is an atypical result inasmuch as normal radiocarbon ages of marine skeletons are progressively younger with increasing age, not older, than U-series ages (Bard et al. 1990). The older ^{14}C ages observed in this study can be reconciled with U-series age only if we conclude that an old source of carbon, such as deep, old, and possibly upwelling waters, sourced the carbon in the skeletal elements.

To offset some of these problems, data were compared internally as outlined below. Further, to our knowledge this is the first time that bryozoans have been used to generate a U/Th stratigraphy, and so several tests were utilized: (1) Both species of *Celleporaria,* from close together in the same core (Hole 1129C), yielded similar results; *Celleporaria* sp. 1 (aragonite) at 54.7 mbsf = 127 ka; *Celleporaria* sp. 2 (LMC) at 56.7 mbsf = 134 ka; (2) *Celleporaria* at the base of unit 3 in 1132B and 1129C at the same depth (90 mbsf) yielded similar ages: 1132B, 90.4 mbsf = 280,508 $\pm$ 6,200 years; 1129C, 90.2 mbsf = 288,000 $\pm$6,100 years. Thus, we conclude that the U-series dates are consistent between species and at specific stratigraphic horizons.

Benthic Foraminifer Stable-Isotope Stratigraphy (Fig. 7).—Stable oxygen isotope variations in the benthic foraminifers *Cibicidoides subhaidingerii, Planulina wuellerstorfi* (both epifaunal), and *Uvigerina peregrina* (infaunal) for the three sites have been reported by Holbourn et al. (2002). The amplitudes of $\delta^{18}O$ fluctuation are low in comparison to $\delta^{18}O$ fluctuations in planktonic or deep-water benthic foraminifers from global deep-water sites (Imbrie et al. 1984; Martinson et al. 1987), but the major differences between glacial and interglacial stages are preserved (Fig. 7).

There is a good correlation between mound units and benthic foraminifers, with high $\delta^{18}O$ values for units 1, 2, and 3, corresponding to MIS 1 to 8 (Fig. 7). The most prominent excursions occur at unit 1–2, 2–3, and 3–4 boundaries and correspond to isotopic shifts between MIS 1 to 2, 5 to 6, and 8 to 9. Values $<$ 1.0‰ occur consistently only in unit 1. Variations within glacial periods is $\sim$ 2.5‰ and within interglacial periods is 1.2‰ to 0.5‰.

Bryozoan Stable Oxygen Isotope Stratigraphy.—Analyses of three bryozoans, two delicate branching, calcitic cyclostomes *Idmidronea* sp. and *Nevianopora* sp. and one flat robust branching aragonitic cheilostome *Adeonellopsis* sp., have similar values when compared to the ranges in the MIS curve (Machiyama et al. 2003).

Sediment Components

Sedimentary particles throughout all three boreholes are a typical cool-water, heterozoan assemblage (James 1997), with skeletal architecture as

←

FIG. 2.—**A)** A north–south seismic section through Sites 1129 and 1131, the eastern transect, illustrating the spatial distribution of mounds. **B)** A north–south seismic section through Site 1132, the western transect, illustrating the spatial distribution of mounds.

TABLE 1.—*Site 1129 unit comparison.*

Unit	Composition[1]	Biota
1	**Burrowed bioclastic gnst,** pkst at base. *Abundant* planktonic and benthic forams, echinoids, pteropods, corallines, ostracods, molluscs, and sponge spic; conspicuous brown benthic foram fragments; *minor* tunicates, pellets, ostracods; *rare* bryos.	Small: 70% bryos (DB, AB), *minor* pteropods, mollusc fragments, echinoids, benthic forams, *Spirorbis.*
2B	UPPER HALF—**Interbedded bioclastic Gnst-Pkst and bryo Flst-Rudst** Gnst-Pkst = fine-grained with pkst in burrows; *abundant* bryos (DB), planktonic and benthic forams, echinoids, corallines; *minor* tunicates, sponge spic, peloids, serpulids, quartz; glauconite near base. Flst-Rdst = rich, grainy, with matrix similar to Gnst-Pkst. LOWER HALF—**Fine grained bryo Gnst and Pkst; Wkst in burrows.** *Abundant* bryo (DB), planktonic and benthic forams, echinoids and corallines, *minor* tunicates, sponge spic, glauconite, and quartz; *local* bivalves, pellets, serpulids, and ostracods.	UPPER HALF Gnst-Pkst = 60–90% bryos, diverse but highly variable; *local* serpulids, large benthic forams, molluscs, pellets, barnacles, echinoids, crab fragments. Flst-Rdst = 60–95% bryos, diverse assemblage, not fragmented, fenestrates vary widely, dominate some intervals; serpulids, gastropods, large benthic forams. LOWER HALF 80–90% bryos, diverse; *minor* serpulids, benthic forams, pellets.
2A	Fine-grained, **burrowed bioclastic Pkst,** particles generally gray, bioeroded; *abundant* bryos (FR, EN, DB), planktonic and benthic forams, corallines, tunicates, quartz (at base) echinoids; *minor* sponge spic, glauconite; *local* serpulids and pellets. *Basal 0.5 m* = a conspicuous unit with all grains fragmented and abraded.	Bryos = 50–90%, diverse but mostly DB with a background of FR&EN; FO present. *Abundant* benthic forams, serpulids; *local* mollusc fragments, pteropods, crab fragments. *Basal 0.5 m* = diverse molluscs (gastropods, pectens, other bivalves), large planktonic forams, <60% bryo.
3B2	**Stacked Flst with Rdst at top, Pkst-Gnst layers near base.** Flst = sparse grainy at top, rich muddy in middle, sparse muddy at base. Matrix = muddy–grainy Pkst. *Abundant* bryo (AB), tunicates; benthic forams; *minor* planktonic forams, echinoids, corallines, sponge spic; quartz and glauconite in upper part; *local* molluscs, serpulids, ostracods. Rdst = like Pkst-Gnst. Pkst-Gnst = muddy bryo-bioclastic; *abundant* bryos (AZ), benthic forams, echionids, tunicates, corallines; *minor* planktonic forams, glauconite, quartz; *local* molluscs, sponge spic.	Flst = 60–100% bryos, diverse, all elements in equal proportions, fragmented only at tops of units, otherwise unbroken. *Abundant* benthic forams, serpulids; *local* pellets, bivalves, barnacles, echinoid spines, gastropods. Rdst = 90% bryos (dominated by FRB, DB, NA, EN); *minor* bivalves, gastropods, serpulids. Particles fragmented and abraded. Pkst-Gnst = bryos = 70–80% (dominated by EN DB) *minor* serpulids, benthic forams, highly fragmented bryos.
3B1	UPPER HALF = **muddy bioclastic Pkst with abraded grains** *abundant* planktonic forams, echionids, *minor* benthic forams, molluscs, corallines, pellets, tunicates, bryos (DB & AZ); *local* glauconite, quartz, sponge spic, intraclasts. LOWER HALF = **basal Gnst/Pkst** with blackened grains overlain by **Flst.** and several fining-upward **muddy, bioclastic Pkst-Wkst** units. Flst = grainy, rich; matrix same as 3B2, but only rare corallines, quartz and glauconite. Wkst-Pkst = *abundant* planktonic forams, benthic forams, tunicates, quartz; *minor* echinoids, corallines, sponge spic.; *local* pellets, molluscs.	UPPER HALF = *rare* bryos, mostly DB. *Local* serpulids and benthic forams. LOWER HALF = Flst —60–100% bryos, totally dominated by DB; rare FRB and AB. Rare gastropods, mollusc fragments; corals at base; grains biodegraded at base. Wkst-Pkst—rare serpulids, benthic forams, molluscs.
3A4	**Massive stacked sparse muddy Flst intervals.** A fe rich muddy Flst & Rdst intervals at top. Matrix = bioclastic muddy pkst, *abundant* tunicates, *minor* benthic forams, sponge spic, ostracods, bryos (AZ); *trace* planktonic forams, quartz; *local* echinoids, corallines, serpulids, glauconite, mollusc fragments.	**Flst**—Bryos = 80–100%, diverse, but dominated by FE, FRB, DB; the EN, NA locally abundant; NA is low, DB is always present and abundant; skeletons unabraded, a few units fragmented. *Abundant* benthic forams; *local* large mollusc fragments, serpulids, *Siliquaria,* olives, and azooxanthellate corals at base.
3A3	Omission surface.	Omission surface.
3A2	A single unit of **sparse muddy Flst** with a rich Flst near base. Matrix = bryo-bioclastic Pkst *abundant* tunicates, benthic forams; *minor* planktonic forams, sponge spic, ostracods; *trace* corallines; *local* serpulids, quartz, bivalves, echinoids.	Bryos = 90–100%; a diverse FFEND assemblage, but few NA (which are small), dominated by FE, FRB, EN, DB. Alternating units of fresh and highly fragmented skeletons; diversity is maximum in middle of unit. *Abundant* benthic forams; *local* serpulids, gastropods, mollusc fragments.
3A1	UPPER HALF = **grainy bryo-bioclastic Pkst** that grades up to Flst of 3A2. *Abundant* bryos (DB), planktonic and benthic forams, echionids, corallines; *minor* tunicates, sponge spic, quartz. LOWER HALF = **grainy bioclastic Pkst** particles highly fragmented and gray. *abundant* pellets, tunicates, ostracods; *minor* bryos (AZ), planktonic forams, corallines, sponge spic, quartz.	UPPER HALF = Bryos = 95–100%, diverse, equal number of types. NA conspicuously small, all highly fragmented. *Minor* echinoids, mollusc fragments (robust and delicate bivalves), pellets. LOWER HALF = similar to upper half but particles not as fragmented.
4C	**Grainy Pkst and capping Gnst** Pkst-Gnst = bryo-bioclastic; *abundant* benthic and planktonic forams, tunicates, bryos (AZ, DB); *minor* echinoids, sponge spic; *trace* corallines, quartz; *local* serpulids; corallines abundant at base, all forams small at base.	Bryos = 90–100% (DB); *minor* benthic forams, serpulids, broken bivalves; gastropods and echinoid spines at base.
4B	**Grainy Pkst and Muddy Pkst with prominent middle Wkst.** Pkst = bryo-bioclastic; benthic and planktonic foraminifers; *trace* corallines, echionid fragments, sponge spicules Wkst = bryo-bioclastic; minor planktonic and benthic forams, tunicates; particles not as diverse as Pkst.	None in wkst.
4A	**Grainy to muddy bioclastic Pkst, burrowed,** *Abundant* bryo fragments, benthic and planktonic forams (small in upper part), corallines abundant at base and top; quartz sand abundant in upper part (particularly between 120 and 125 mbsf); *minor* echinoids, tunicates, sponge spic; *trace* ostracods, peloids. **cm-thick layers of Gnst or Flst,** similar composition.	Bryos = 70–100%, variable but dominated by DB, locally high in fragmented NA, VA, FRB; *local* serpulids, bivalves, pellets (lithified) crab fragments, echinoid fragments, gastropods.
5	UPPER HALF = **Grainy to muddy bioclastic Pkst with thin sparse muddy Flst layers and at top**; capped by omission surface. Pkst = *abundant* benthic and planktonic forams, tunicates; *minor* bryos (AZ), sponge spic, quartz; *local* echinoids, molluscs, serpulids, ostracods. Flst matrix = *abundant* benthic and planktonic forams; *minor* bryos (AZ), tunicates, sponge spic, quartz; *local* echinoids, corallines; *trace* ostracods. LOWER HALF = **massive, burrowed, muddy, bryo-bioclastic Pkst** *abundant* benthic and planktonic forams, bryos (AZ), sponge spic.; *minor* echinoids, corallines, tunicates, quartz; *local* serpulids, molluscs, ostracods, very small planktonic and benthic forams.	UPPER HALF = **Pkst**—*minor* bivalves, benthic forams, serpulids, lithified pellets, bryos cemented, encrusted, highly fragmented. **Flst** = Bryos dominated by FE, NA with highly variable numbers of EN, DB, all fragmented. *Minor* bivalve and benthic foram fragments. LOWER HALF = Bryos = 10–90%; diverse and highly variable but always containing FE, FR, DB. *Abundant* degraded and abraded bryos, pellets, echinoid spines, benthic forams, azooxanthellate corals; *local* bivalves.

[1] Abundant = >10%; Minor = <10%; Trace = <5%; Local = abundant in specific units; bryo = bryozoan; foram = foraminifer; spic = spicule. Flst = Floatstone; Rdst = Rudstone; Gnst = Grainstone; Pkst = Packstone; Wkst = Wackestone. Bryo Growth Forms (from figures with growth form data).

the principal determinant of particle size. This is dependent upon growth form in bryozoans, with some skeletons generating coarse pieces, others fragmenting into sand-size particles, and still others spontaneously disintegrating into mud-size elements (cf. Bone and James 1993; James et al. 2001).

Coarse biofragments > 1 mm are generally bryozoans (Fig. 9), with bivalves, gastropods, serpulid tubes, echinoid spines and plates, fecal pellets, and barnacle plates locally abundant but rarely totaling more than 10% by volume. Benthic foraminifers (agglutinated, rotalid, miliolid, and hyaline) are common whereas planktonic foraminifers are rare.

Sand-size grains are mostly benthic and planktonic foraminifer tests, serpulid worm tube fragments, bryozoan pieces, whole and fragmented individual zooids (singlets) of articulated zooidal bryozoans, whole and fragmented molluscs, and soft to hard fecal pellets. Other common but variable biofragments are echinoid spines and plates, azooxanthellate corals, and coralline algal rods and pieces. Smaller particles (bryozoan pieces, ostracods, foraminifers, infaunal echinoid spines; Fig. 10A, B) are also common in the carbonate mud together with tunicate spicules, siliceous sponge spicules, bioclasts eroded by boring sponges (sponge chips), minor pteropods,

TABLE 2.—*Site 1132 unit composition.*

Unit	1132 Composition[1]	1132 Biota
1	Coarse sorted **gnst** to **pkst.**	Abraded bryos, diverse conspicuous FRB, DB; large benthic forams, pectens, olives.
2B	Massive **flst-rdst**; muddy–grainy flst layers grading upward to rdst layers; burrowed.	Rich and diverse bryo assemblage; conspicuous AB, FEN, FRB. *other particles* = serpulids, *Siliquaria*, epifaunal echinoid spines, large benthic forams. Some layers contain numerous gray bioeroded grains; clypeasters in rdst.
p	LOWER HALF = grainy **pkst,** burrowed. UPPER HALF = grainy **pkst** and sub-meter-thick **flst.**	LOWER HALF = high proportion of fragmented bryos, serpulids, gastropods, bivalves; the capping grainy flst contains prolific FRB bryos. UPPER HALF = FEN bryos common; numerous AB in flst; abraded.
3B2	Lower **flst** = burrowed. Middle muddy **pkst.** Upper **flst** = sparse.	Lower **flst**—diverse bryo assemblage, numbers and diversity increase upwards, but low at top, where many pieces fragmented. Upper **flst** = rich and diverse bryo biota; most abundant in all of unit 3.
3B1	Poorly sorted muddy **pkst** with local thin and sporacid flst.	
3A4	Massive stacked **flst.** as in 1129, conspicuously burrowed.	Bryo diversity not as high as 1129.
3A3	LOWER = **muddy pkst** with lithified peloids grading upward to sorted **pkst**; capped by prominent lag. UPPER = muddy **pkst,** numerous DB bryos, *Dentalium,* crab fragments, large forams, abraded bryos at top.	Common bivalves and large benthic forams.
3A2	Grainy to sparse muddy **flst,** numerous fragmented DB bryos at base but more diverse upward; numerous gastropods, bivalve fragments and occasional whole brachiopods in lower half.	
3A1	Muddy–grainy **pkst** with numerous blackened broken and abraded grains.	
4C	Light-colored pkst with 1–3 m-thick **gnst** units.	Cemented peloids and intraclasts throughout; LOWER PART = numerous DB bryos; UPPER PART = fewer bryos and more fragmented biodegraded and abraded bivalves, serpulids, corals, and benthic forams; intraclasts common above omission surfaces.
4B	Muddy **pkst** with one middle unit of **wkst.**	Bryos in pkst = DB; in wkst AZ; grains not gray and biodegraded.
4A	Muddy **pkst**; burrowed, numerous omission surfaces.	Bryos = DB; lithified peloids, coarse layers contain DB bryos, broken *Dentalium,* molluscs: grains overlying omission surfaces gray and biodegraded.
5	LOWER HALF = fine **pkst.** UPPER HALF = **flst** layers: meter-scale turbidites.	Bryos = all elements, but dominated by DB.

[1] Abundant = >10%; Minor = <10%; Trace = <5%; Local = abundant in specific units; bryo = bryozoan; foram = foraminifer; spic = spicule; Flst = Floatstone; Rdst = Rudstone; Gnst = Grainstone; Pkst = Packstone; Wkst = Wackestone. Bryo Growth Forms (from figures with growth form data).

TABLE 3.—*Site 1131B unit composition.*

Unit	1132 Composition[1]	1132 Biota
1		
2B3	Rich, grainy **Flst** with minor **Rdst** an pkst gnst Flst matrix = muddy Pkst, *abundant* brown bioclasts, *minor* planktonic forams, ostracods, *local* benthic forams, tunicate spic., sponge chips. Gnst = peloid bryozoan bioclasts; *abundant* large pellets, bryo, benthic forams, small ostracods; *minor* small, planktonic forams; *local* sponge spic., quartz.	95–100% bryos (FE, FR, EN, NA, DB); local serpulids and fragmented bivalves.
2B2	Sub-m-scale layers of **Pkst, Wkst** and rich muddy **Flst.** Pkst = 1/2 peloid-bryo pkst with *abundant* pellets, bryo, minor planktonic and benthic forams, serpulids; 1/2 bioclastic Pkst = *abundant* brown bioclasts, benthic forams; *minor* planktonic forams, sponge spic., ostracods, and *local* echinoids, corallines.	80–90% bryo (FR, NA dominant); skeletons worn and abraded; common sponge spicules; local layers with 70% serpulids; fragments of bivalves and gastropods; occasional conspicuous large planktonic forams and pteropods.
2B1	Meter-scale interbedded sparse grainy **Flst** and **Rdst** Matrix = grainy peloid pkst with *abundant* pellets, bryo and benthic forams, and grainy pkst with *abundant* brown bioclasts, corallines, tunicates, sponge spicules, ostracods, sponge chips, and benthic forams; *minor* planktonic forams.	80–100% bryos; diverse but few NA and numerous FE; layers either diverse or DB dominated; serpulids at base; delicate bivalves throughout; serpulids at base; local gastropods, brachiopods, and crab claws.
2A	Grainy **Pkst** with *abundant* brown bioclasts, ostrapods; *minor* peloids, benthic forams, planktonic forams; *local* corallines, echinoids.	A miniscule fraction of worn and abraded bryos and bivalve-gastropod fragments.

[1] Abundant = >10%; Minor = <10%; Trace = <5%; Local = abundant in specific units; bryo = bryozoan; foram = foraminifer; spic = spicule. Flst = Floatstone; Rdst = Rudstone; Gnst = Grainstone; Pkst = Packstone; Wkst = Wackestone. Bryo Growth Forms (from figures with growth form data).

and prolific coccoliths (Fig. 11). The only nonskeletal grains are rare quartz particles and glauconite.

All floatstone particles are typically whole and appear fresh, with some fragmented, likely through predation, but rarely abraded. In contrast, bedded sediments can be composed of eroded and abraded particles, which may be gray to black and bioeroded. Sediment particles throughout may have isolated crystals to irregular rinds of calcite cement, but such cement is conspicuous only below 90 meters below sea floor (mbsf). Similarly, peloids are friable to hard only below this depth. Burrows have the characteristics of decapod crustacean dwelling sites (cf. *Thalassinoides*) but are poorly preserved.

Sediment is characteristically muddy, unlithified, biofragmental, and rich in bryozoans, with texture varying from floatstone to wackestone (Fig. 10; Tables 1, 2, 3). Differences in texture can be subtle, especially between a sparse floatstone, and a fine-grained packstone with a few large bryozoan fragments. Deposits are usually in the form of meter-thick floatstone units separated by similar-scale units of packstone. Sediment is heterogeneous even at the small scale, with packstone in centimeter-thick layers or as burrow fillings.

Paleontology

Bryozoans.—Bryozoans are identified to the generic level and are currently under detailed study (Bone and James 2002). There are a maximum of 96 genera (Appendix 1, see Acknowledgments) grouped under nine growth forms (cf. Bone and James 1993). Although the majority of genera have a single growth form, several genera exhibit different growth forms because of their ''plastic'' growth habits that change through life. The most ubiquitous forms are fenestrate, flat robust branching, encrusting, nodular–arborescent, and delicate branching (Fig. 12), herein called the FFEND assemblage. All these growth forms tend to be dominated by a few genera, except for encrusting types, which exhibit high generic diversity.

Fenestrate bryozoans are not diverse with the four important genera, *Iodictyum, Reteporellina, Sertella,* and *Triphyllozoon,* of roughly equal importance. Flat robust branching forms are more diverse, with *Adeonellopsis, Bracebridgia, Caleschara, Labioporella,* and *Porina* being most abundant. Delicate branching forms are likewise fairly diverse and dominated by *Idmidronea, Nevianipora,* and *Hornera.* Foliose, vagrant-pseudovagrant, articulated branching, and articulated zooidal forms have several important but no dominant genera. Nodular–arborescent types, although conspicuous because of their large size, are not diverse and dominated by *Celleporaria.*

The fine fraction contains generally the same genera together with two foliose growth forms. The main difference is, as expected, the very large numbers of delicate branching, articulated branching, and articulated zooidal forms. Except for the delicate branching, which are formed by large numbers of *Idmidronea* and *Nevianopora,* growth forms are of moderate diversity.

Planktonic Foraminifers.—Planktonic foraminifers are mostly typical

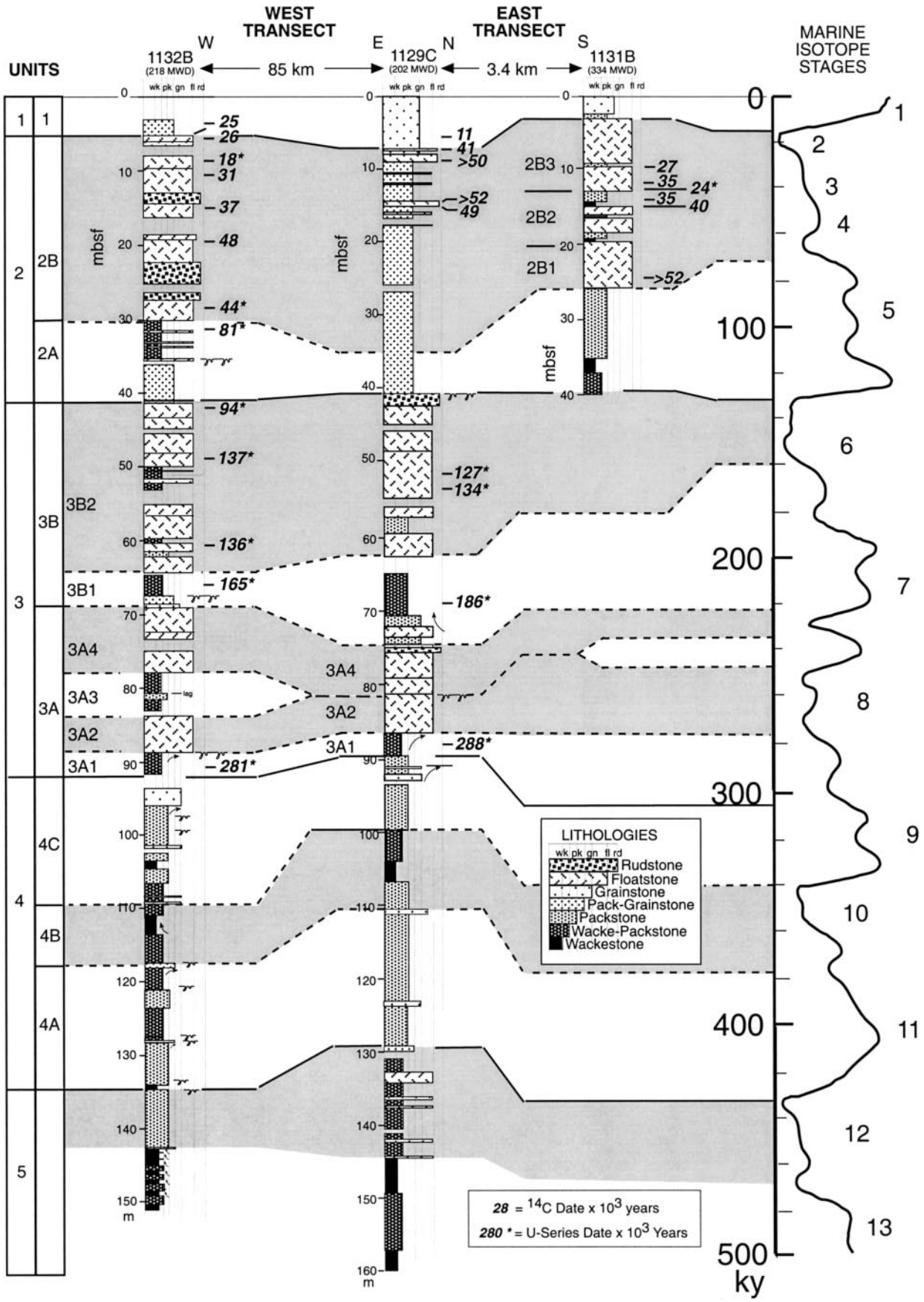
WEST TRANSECT
EAST TRANSECT
UNITS
W
E
N
S
1132B
(218 MWD)
85 km
1129C
(202 MWD)
3.4 km
1131B
(334 MWD)
wk pk gn fl rd
MARINE ISOTOPE STAGES
mbsf
m
ky
2B3
2B2
2B1
3B2
3B1
3A4
3A3
3A2
3A1
lag
LITHOLOGIES
Rudstone
Floatstone
Grainstone
Pack-Grainstone
Packstone
Wacke-Packstone
Wackestone
28 = 14C Date x 10^3 years
280 * = U-Series Date x 10^3 Years

southern mid-latitude forms (Li et al. 1999), with diversity varying between 10 and 20 species. The assemblage comprises abundant (> 30%) *Globorotalia inflata,* and common (5–20%) *Globigerina bulloides, G. falconensis, G. quinqueloba, Globigerinoides ruber,* and *Globorotalia truncatulinoides.* Less abundant (< 5%) forms are *Neogloboquadrina dutertrei, N. pachyderma, Orbulina universa, Globorotalia hirsuta,* and *Globigerinita glutinata.* Among the common forms, *G. inflata, G. bulloides,* and *G. quinqueloba* are cool-water indicators, typically related to upwelling (Almond et al. 1993). *Globigerinoides ruber* is a warmer-water species, as are those which are sporadic. Deep-water dwellers are represented by *G. truncatulinoides,* a species capable of living below the thermocline at depths of 50 to > 1000 m (Hemleben et al. 1989).

Abundance ratios of planktonic foraminifers were analyzed at Sites 1131 and 1132. Several trends emerge when the percentage of planktonic foraminifers, the number of planktonic species, and the ratio between *Globigerinoides ruber* and the three cool-water indices *Globorotalia inflata* + *Globigerina bulloides* + *Globigerina quinqueloba* (abbreviated as ''the ruber ratio''), are plotted against stratigraphic depth. Both the percentage of planktonic foraminifers relative to their benthic counterparts, and the number of species, increase with depth at both sites, reflecting upward shallowing and overall progradation. The variability in the ruber ratio, however, clearly indicates fluctuating water masses that can be tied to the marine isotope stages.

At Site 1131B unit 1 (MIS 1; Fig. 8), with high numbers of planktonic foraminifer species and a high ruber ratio represents a period of relatively warm oligotrophic conditions (cf. Li et al. 1999). Unit 2 bryozoan rudstones and floatstones between 3.5 and 25 mbsf, (MIS 2 and 3; Fig. 8), is an interval characterized by abundant *Gr. inflata, G. bulloides,* and *G. quinqueloba.* In deeper intervals, although *G. inflata* still predominates, *Gs. ruber, Globigerinoides trilobus* s.l., *Globorotalia* spp., and other warm-water species increase significantly in numbers, indicating warm, nearly oligotrophic conditions during MIS 5, early MIS 3, and MIS 4.

Planktonic foraminifers are rarer at the shallower water Site 1132B. In units 1 through 3, abundance fluctuations occur near mean intervals of 30–80% and 15–30% respectively. Abundance values of 50% or more are consistent in sub-mound units 4 and 5. The low abundance of the total planktonic fauna, low diversity, and low ruber ratio are coupled with high dominance of cool-water species *G. inflata, G. bulloides,* and *G. quinqueloba,* which indicates cool periods corresponding to even-numbered isotope stages. In contrast, a high faunal abundance, high diversity, and high ruber ratio imply warm conditions at odd isotope stages. The ruber ratio is consistently higher across units 3 and 4 (MIS 7 to 9), possibly related to an unusual local environment at the time of transition to more euphotic conditions and development of larger-scale mounds.

Benthic Foraminifers.—There are two distinct benthic foraminifer assemblages (Holbourn et al. 2002). The first, a *Panulina wuellerstorfi* assemblage, is usually associated with somewhat oligotrophic conditions and is characterized by *P. wuellerstorfi, Eherenbergina pacifica, Gyroidina orbicularis, Cancris auriculus, Elphidium macellum,* and *Lenticulina* spp. The second, a *Bulimina marginata* assemblage, indicative of mesotrophic conditions, typically contains *B. marginata, Bigeneria nodosaria, Patellina corrugata, Cornuspira foliacea, Oridorsalis umbonatus,* and *Globulina* spp. A large number of species occur in both assemblages (Holbourn et al. 2002), including *Cibicidoides subhaidingerii, Astrononion pussillum, Discoanomalina coronata, Globocassidulina subglobosa, Hoeglundina elegans, Loxostomina* sp., *Siphogenerinoides* sp., *Textularia* spp., and various miliolids.

Stratigraphic Sedimentology

Attributes of the sediment and variations in the bryozoan biota for each unit and subunit are illustrated in Figures 13 to 20 and detailed in Tables 1 to 3.

Unit 5 (Fig. 13).—This is the deepest unit with significant bryozoan fragments. It is characterized by peri-mound sediments that are seismically well stratified and occur downslope from extensive, older mounds (Figs. 4, 6). The unit is capped by a prominent omission surface at Site 1132B. This omission surface, like all omission surfaces in the cores, is characterized by intense burrows and a sharp upper boundary. Lower packstones and local wackestones (MIS 13, highstand) are massive and burrowed at Site 1129, but at Site 1132 are graded at the meter-scale, indicating that they are calciturbidites. The allochthonous particles are fragmented, abraded, and biodegraded. Most grains are lithified pellets, small planktonic and benthic foraminifer tests, and articulated zooidal bryozoan singlets, with numerous sponge spicules and a few coralline algae. The algal fragments attest to minor but continuous offshelf transport. Upper grainy to muddy packstones (MIS 12, lowstand) are similar but rich in tunicate (particularly ascidian) spicules, poor in bryozoan fragments, and devoid of corallines. Coarse floatstone bryozoans, which occur only in 1129C, although diverse, are dominated by encrusting, nodular–arborescent, and delicate branching forms (Fig. 14). Coarse bryozoans in packstones from both units are dominated by delicate branching forms.

Unit 4 (Fig. 13).—These grainy sediments lie downslope from any mounds and are composed mostly of muddy to grainy packstone with dispersed bryozoans. The sediments are divisible into three subunits; a lower grainy packstone (unit 4A), a middle packstone with a prominent wackestone in the center (unit 4B), and an upper mostly grainy packstone (unit 4C). These subunits are correlated with MIS stages 11, 10, and 9, respectively (Figs. 3, 7). All sediment, like unit 5, is rich in benthic and planktonic foraminifers and contains numerous delicate branching bryozoan fragments (Fig. 14). There is good agreement between core lithologies and seismic facies except for the upper parts of 1129, which are peri-mound to mound-flank, seismic facies but appear to be all peri-mound in core.

Unit 4A comprises decimeter, fining-upward, muddy to grainy packstone layers (interpreted as calciturbidites) to homogeneous layers with conspicuous peloids and gray biodegraded grains. Quartz grains are prominent in the upper half of 1129, whereas 1132 contains conspicuous burrowed omission surfaces. The unit is capped a grainstone with a prominent burrowed omission surface in 1132 and a floatstone dominated by fresh-appearing autochthonous, delicate branching bryozoans, implying a deep-water origin in 1129.

The muddy to grainy packstones of unit 4B contain many fewer biodegraded grains than 4A, but most bryozoans are still delicate branching. The wackestone in the center, two to three meters thick, is white to pale yellow with few biofragments except for rare articulated bryozoan zooids, tunicates, and small foraminifers. These two lithologies suggest little offshelf transport.

Unit 4C is overall similar to unit 4A, with decimeter fining-upward calciturbidites and local burrowed omission surfaces but not much quartz. These lithologies and their similarity to unit 4A support an overall peri-mound facies interpretation.

Unit 3 (Fig. 15).—This ~ 50 m-thick unit is similar bryozoan floatstone at both sites with more packstone layers at Site 1132. A package of muddy packstone at ~ 65–70 mbsf separates the unit into two parts, here designated units 3A and 3B. Unit 3A is further subdivided into subunits 1

←

FIG. 3.—A correlation diagram of lithologies in Sites 1132, 1129, and 1131. Lithologic units are designated at left and correlation with marine isotope stages (MIS) at right. Radiometric age dates are in bold italics (Appendix 2). Gray-shaded intervals denote glacial periods, when sea level was low.

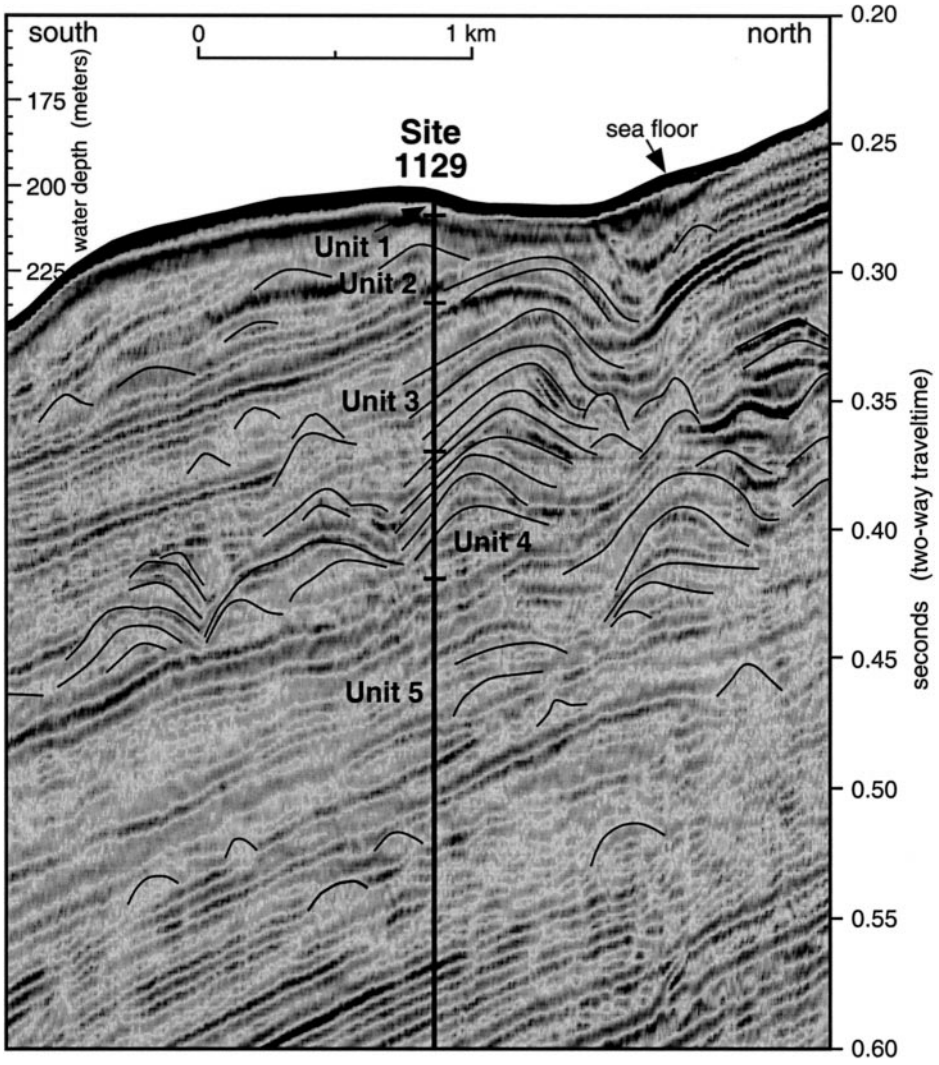

FIG. 4.—A detailed seismic section of Site 1129 illustrating location of the various lithostratigraphic units shown in Figure 3. Positions of mounds are interpreted from seismic facies noted elsewhere.

through 4, reflecting alternating meter-scale packstone and floatstone lithologies. These subunits are correlated between sites, with unit 3A3 in 1132B interpreted to be represented by an omission surface in 1129C. Unit3B is subdivided into two subunits, a lower packstone-rich lithology and an upper floatstone-rich lithology. Unit 3 is correlated with MIS 8, 7, and 6 (Fig. 3). There is good agreement between seismic facies (Figs. 4, 6) and lithological facies (Fig. 13) for unit 3 in 1132, with mound-core, mound-flank, and peri-mound facies all represented. There is also correspondence between seismic and core lithologies for units 3A and 3B1 in 1129, with both indicating mound-flank facies overlain by inter-mound facies. Unit 3B2 in 1129, however, is peri-mound on seismic but looks to be more mound-flank in core (but with numerous highly fragmented bryozoans at the top), suggesting that it may be the margin of a broad mound.

Subunit 3A1, a muddy packstone (Fig. 15), is rich in allochthonous fragmented, bioeroded, and locally blackened biofragments, particularly bryozoans, planktonic and benthic foraminifers, echinoids, and coralline algae. Equal proportions of the FFEND assemblage (Fig. 16) suggest derivation from upslope mounds. It is correlated with an intermediate-level highstand early in MIS 8. Muddy packstones of subunit 3A3 at Site 1132 can be correlated with the early MIS 7 highstand (Fig. 3), but resolution is not sufficient to tell for certain. They contain lithified peloids, fragmented and cement-filled bryozoans, bivalves, and large ($>$ 1 mm) benthic foraminifers. Sediment in unit 3A3 is interpreted to be largely allochthonous. The interpreted coeval omission surface, which is evidenced by a sharp surface and prominent burrows and correlated with subunit 3A3 at Site 1129, is thought to be due to nondeposition and possible seafloor erosion.

Subunits 3A2 and 3A4 are floatstones that are correlated with the overall MIS 8 lowstand and a lowstand in early MIS 7 (Fig. 3). Lithologies are interpreted to represent active mound growth with a diverse bryozoan population but distinguished by relatively low numbers of nodular–arborescent forms (Fig. 16). Finer sediments here are characterized by prolific tunicate spicules and local, abundant, large (over 1 mm) benthic foraminifers. The 3A–3B contact, immediately overlain by epifaunal biofragments, blackened and fragmented grains, and an omission surface in 1132, represents arrested sedimentation interpreted to be associated with rapid MIS 7 sea-level rise.

Subunit 3B1 is interpreted as representing late MIS 7 highstand deposition, with the basal quartzose, tunicate-rich sediment containing abundant planktonic and benthic foraminifers recording transgression and the overlying muddy packstones with abundant planktonic foraminifers representing prolonged highstand. Bryozoans are dominated by delicate branching forms (Fig. 16). Subunit 3B2 bryozoan diversity and richness (Fig. 16), correlated with MIS 6 lowstand (Fig. 3), imply active mound growth with stacked floatstones confirming seismic interpretations (Figs. 4, 6) of mound-flank facies in 1132. These are amongst some of the most diverse and bryozoan-rich floatstones. Abraded biofragments at the top suggest reduced sedimentation and possible reworking by waves and swells.

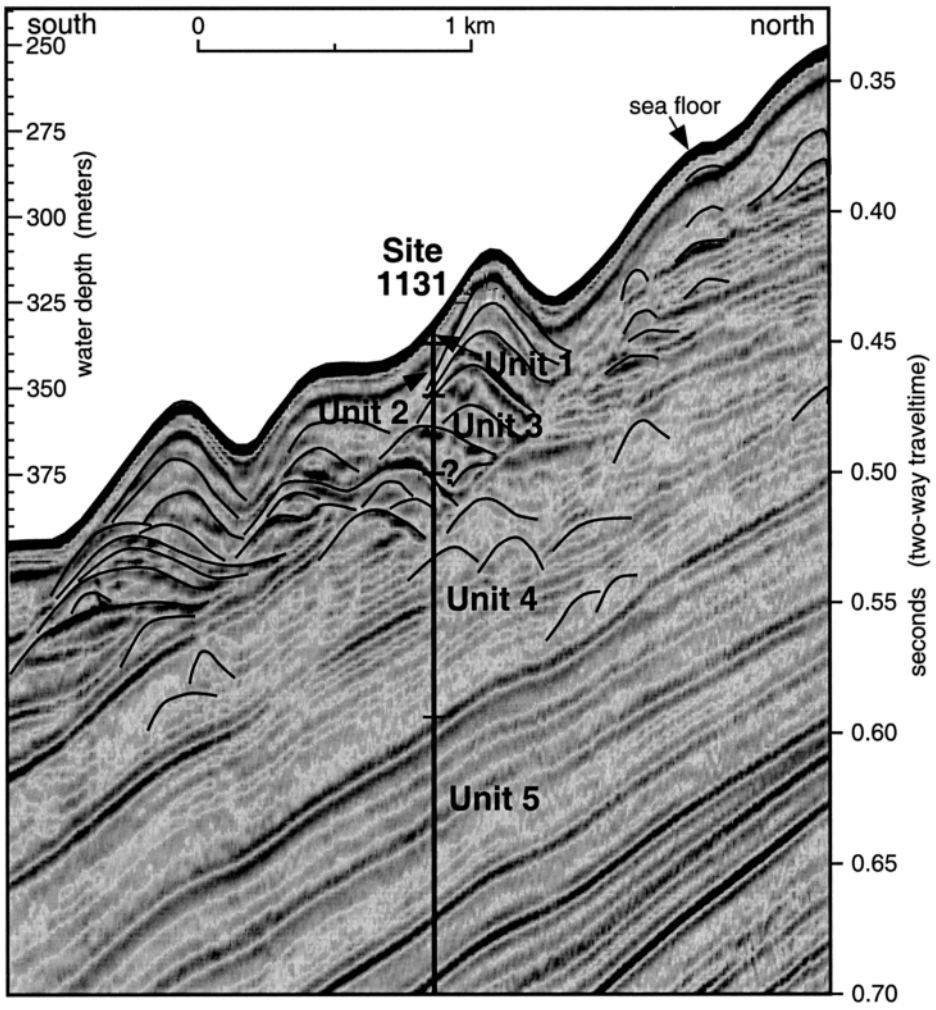

FIG. 5.—A detailed seismic section of Site 1131 illustrating location of the various lithostratigraphic units shown in Figure 3. Positions of mounds are interpreted from seismic facies noted elsewhere.

Unit 2—Upslope Mounds (Fig. 17).—The basal contact of unit 2 is sharp at Site 1132 and separated from unit 3 by a clear burrowed omission surface at Site 1129. The unit is divided in 1132B into unit 2A, a grainy and muddy packstone, and unit 2B, mainly floatstone and rudstone. Separation is not as clear in 1129C, where most sediment is grainy packstone. Grainy sediments of subunit 2A are correlated with MIS 5 highstand (Fig. 3). The upper part of unit 2 at Site 1129 is eroded and confirmed by ^{14}C dates with a gap of 30 ky at about 7 mbsf (Fig. 3). This surface is not obvious on seismic (Fig. 4). There is fair agreement between seismic (Figs. 4, 6) and core (Fig. 17) for unit 2A, but unit 2B correlates poorly. Unit 2B is lithologically mound core to mound flank in 1132 but peri-mound in seismic facies. In 1129 unit 2B is peri-mound with an interpreted small mound core on seismic but lithologically peri-mound in core.

The deposits of unit 2A are interpreted, on the basis of extensive fragmentation and bioerosion, to be allochthonous. All of unit 2A is rich in planktonic and benthic foraminifers, coralline algae, tunicates, quartzose sand, and blackened grains. Large planktonic foraminifers in unit 2A at Site 1129 confirm warm surface waters, supporting a correlation with MIS 5. Bryozoans are diverse, with numerous flat robust branching and delicate branching forms (Fig. 18). Floatstone layers at Site 1132 are rich in abraded arborescent bryozoans.

Numerous geochemical dates from unit 2B allow the sediments to be directly correlated with MIS 2, 3, and 4 lowstands (Fig. 3). Sediments are different at the two sites, floatstone and rudstone at Site 1132, grainy packstone with minor floatstone at Site 1129. The overall lack of abraded material in the packstones of Site 1129 suggest minimal transport, corresponding to a peri-mound, but mound growth immediately upslope. Meter-scale floatstone–rudstone cycles at Site 1132 likely represent rapid accretion and local senescence, followed by renewed growth. Sediments are rich in bryozoans, foraminifers, echinoids, and corallines in both packstones and floatstones; bryozoans are generally diverse and comprise all forms of the FFEND assemblage (Fig. 18).

Unit 2—Downslope Mounds (Fig. 19).—These buildups were cored at two localities, 40 m apart in water depths of 331.4 mwd (1131B) and 333.4 mwd (1131A), and they illustrate the rapid lateral facies changes present in zones of mound growth (Fig. 19). Such rapid changes are likely, in part, responsible for the poor correlation between seismic and lithological facies in some units. Radiometric age dates indicate that these mounds also grew during MIS 2, 3, and 4. Seismic images (Fig. 5) show that coring penetrated mound and mound-flank lithologies. Sediments are not significantly different from upslope mounds, with floatstone matrix typically a soft pellet packstone. Sediment between is fine-sand-size muddy bioclastic packstone with abundant planktonic and benthic foraminifers, brown biofragments, and small broken ostracods and foraminifers, with locally abundant sponge spicules and corallines. Although most particles show little breakage, grainy sediments are locally highly fragmented and abraded. Burrowed omission surfaces are present at the tops of some intervals. Overall, bryozoans in floatstones have: (1) higher diversity; (2) larger and more diverse encrusting forms; and (3) higher numbers of foliose forms (more *Calescharа*, than coeval shallower mounds (Fig. 20).

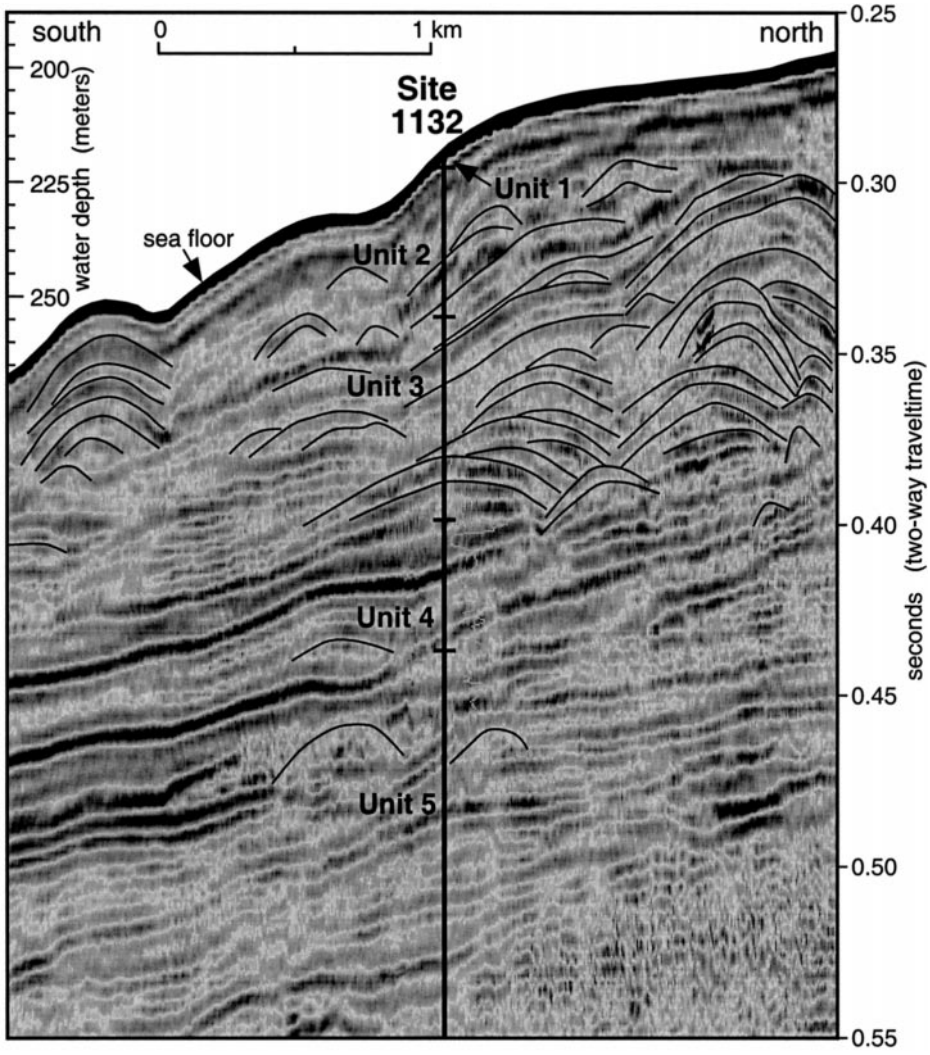

FIG. 6.—A detailed seismic section of Site 1132 illustrating location of the various lithostratigraphic units shown in Figure 3. Positions of mounds are interpreted from seismic facies noted elsewhere.

Unit 1 (Fig. 17).—This < 10-m-thick Holocene burrowed bioclastic packstone and grainstone blankets all mound and intermound areas and is contiguous with the modern seafloor. Conspicuous amongst the grains are brown miliolid foraminifer fragments and delicate and articulated branching bryozoans. These deposits accumulated during the last postglacial rise in sea level and lie in the zone of modern downwelling (James et al. 2001). They are contiguous with seafloor Facies SB (Spiculitic, Branching Bryozoan Mud; 100–200 mwd) and Facies M (Spiculitic Mud; 200–350 mwd+) of James et al. (2001).

Sedimentation Rates.—On the basis of mound unit thicknesses and associated age dates, lowstand mounds grew at rates of 30–67 cm/ky whereas highstand, intermound facies accumulated more slowly at 17–25 cm/ky. Such rates are somewhat less than rates of Holocene sediment accumulation on the Otway margin (upper slope, 2–50 cm/ky; mounds, 105 cm/ky; Boreen and James 1993). The rates determined here for longer periods are, however, probably better estimates for this environment, because they incorporate growth, erosion, and local mass wastage, processes not included in the Holocene rates.

DISCUSSION

Mound Architecture

Seismic images show upslope stacked mound complexes underlying the uppermost slope at ~ 200 mwd in both drilled transects (Figs. 2, 4, 6) and downslope stacked mound complexes on the eastern transect at ~ 300–400 mwd (Figs. 2, 5). These mound complexes are a complicated heterogeneous array of buildups and intermound sediment, indicating growth in response to both allogenic (e.g., eustasy, oceanography) and autogenic (e.g., position on slope, inherited topography) factors.

As noted previously (James et al. 2000), mounds occur in this general geomorphic position throughout the Pliocene–Pleistocene, through several hundred meters of stratigraphic section, implying that conditions suitable for mound growth have been present intermittently along this margin for the last five million years. Because the succession is prograding, the section recorded at the drill sites is overall shallowing-upward. But the pattern is not simple. Everywhere the structures are broad low-relief features that, despite growth within a markedly progradational succession, show principally aggradational to slightly retrogradational geometries: once nucleated they tended to migrate upslope somewhat (Figs. 4, 5, 6), especially during the late Pleistocene. Coupled with development of mound or mound-flank facies only in association with lowstand MIS (Fig. 3), such geometries imply that during a specific growth episode buildups grew vertically during lowstand but terminated as conditions changed during sea-level highstand. During the following lowstand, mounds appear to have nucleated either on preexisting highs (buried mounds) or stepped downslope to new locales.

The Quaternary portion of the prograding carbonate wedge can be divided into two mound growth phases: (1) a long, early to middle Pleistocene (1.7–0.3 Ma) phase of scattered but persistent buildup growth with

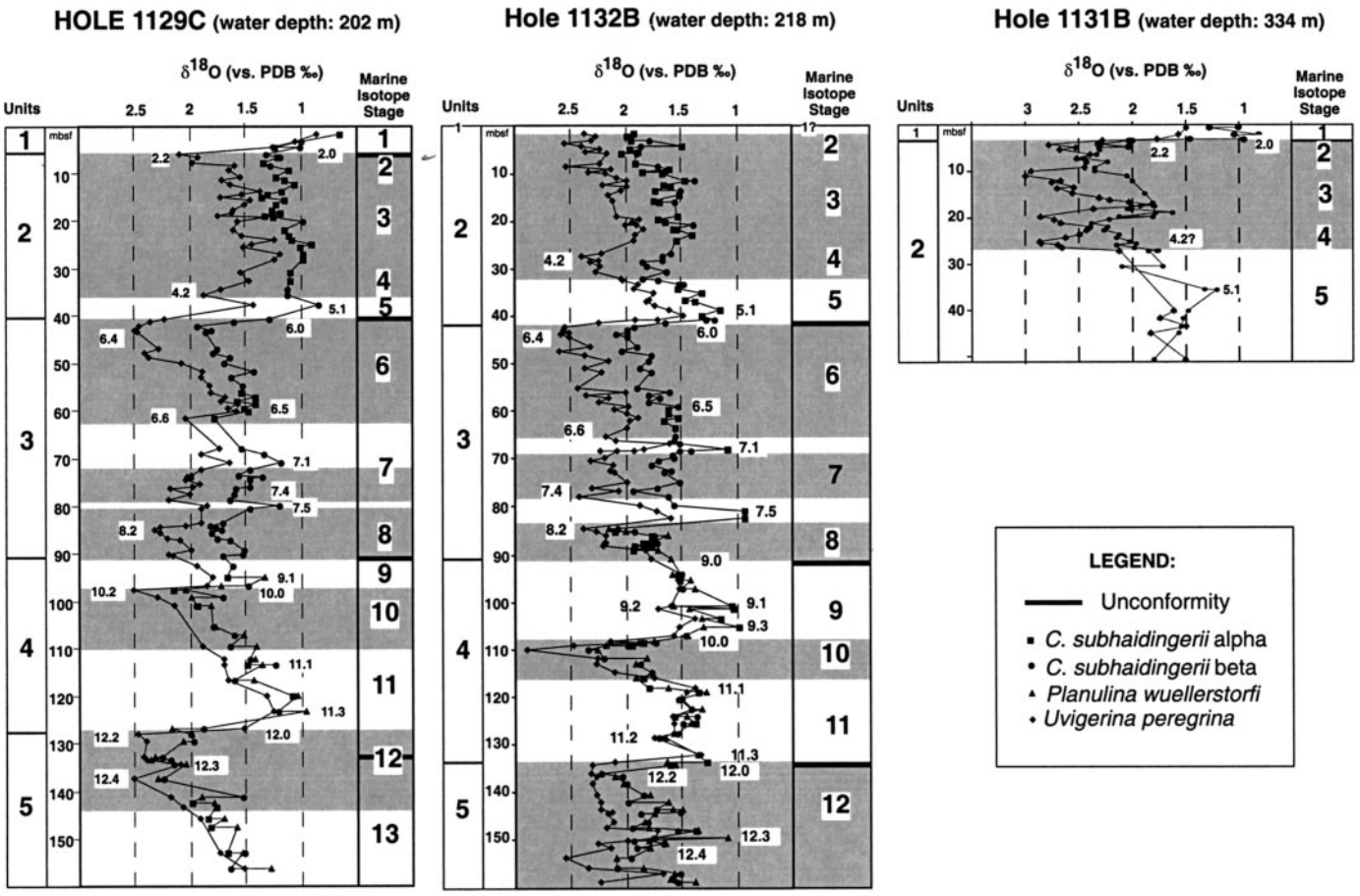

FIG. 7.—Oxygen isotope composition of four benthic foraminifers in bryozoan-rich units from Sites 1129, 1132, and 1131. Gray-shaded intervals denote glacial periods, when sea level was low. MIS substages (e.g., 2.2, 4.2, 5.1, etc.) after Prell et al. (1986).

more retrogradational geometry (Fig. 2); and (2) a shorter, late Pleistocene (< 0.3 Ma), units 2 and 3, phase of extremely active, mostly aggradational growth. Mounds grew actively at several depths along the margin during the very latest Pleistocene part of this second phase (Figs. 4, 5, 6).

These mounds may extend across much more of the southern Australian margin than explored by this study. Specifically, mound surfaces are now exposed by erosion at the seafloor in 250–300 mwd (^{14}C ages of 14–21 ka) in the eastern GAB (James et al. 1997), ~ 500 km east of the drill sites. Late Pleistocene mounds (^{14}C ages 17–18 ka) underlying a thin veneer of Holocene slope sediment have also been piston cored on the upper slope of the Otway margin (approximately 1200 km east of the central GAB) at 280 and 333 mwd (Boreen and James 1993).

Mound Biota

Bryozoans have wide environmental tolerances and so are seldom restricted to distinct environments, but they tend to dominate in specific settings (Hageman et al. 1997). The FFEND assemblage reflects both setting and time of growth. There are 73 genera in deeper-water Site 1131 mounds and 78 genera in the Site 1129 shallower-water mounds (Appendix 1, see Acknowledgments). Most growth-form groups are composed of the same genera, except that shallower mounds contain more articulated branching and articulated zooidal genera, whereas deeper mounds have a somewhat higher diversity of encrusting types, albeit in low abundances. These trends reflect: (1) the globally high proportion of encrusting growth forms in Neogene environments (McKinney and Jackson 1989); (2) the propensity for the ratio of encrusting/erect forms to increase with depth (McKinney and Jackson 1989); and (3) the likelihood that this environment was conducive to epizooidal growth (cf. Hageman et al. 2000). Seafloor photographs of modern upper-slope environments in this area show prolific growth of bryozoans on ephemeral biological substrates such as other bryozoans, sponges, hydroids, and tunicates (James et al. 1992; James et al. 1997; James et al. 2001).

Regardless of stratigraphic unit, the histograms in Figures 14, 16, 18, and 20 indicate that the coarse fraction in floatstones consistently averages 10–25% of large growth forms (fenestrate, flat robust branching, and encrusting) except for nodular–arborescent, which average 5–20% and are highly variable within and between units. Smaller, delicate branching forms are also prolific, averaging 20–30% of the biota. Articulated branching forms are relatively low, likely because they are adapted to shallower, energetic paleoenvironments (Bone and James 1993). Inter-mound and peri-mound packstones have proportionally fewer large forms (5–20%) but more delicate branching forms (25–40%), probably reflecting both *in situ* growth and the fact that the light, delicate branching skeletons are more easily transported.

These growth forms are all present in modern upper-slope environments in southern Australia (Bone and James 1993; Hageman et al. 1996, 1997; Hageman et al. 2000). Fenestrates are most plentiful in waters shallower than ~ 130 m, flat robust branching and encrusting forms extend deeper, to ~ 200 mwd, and nodular–arborescent forms are deep-water bryozoans, being abundant between 120 and 250 mwd. *Celleporaria* thickets, however, thrive within a narrow environmental range in the Cenozoic and Recent of southern Australia, namely below sub wave base (< 120 mwd), on a mud–

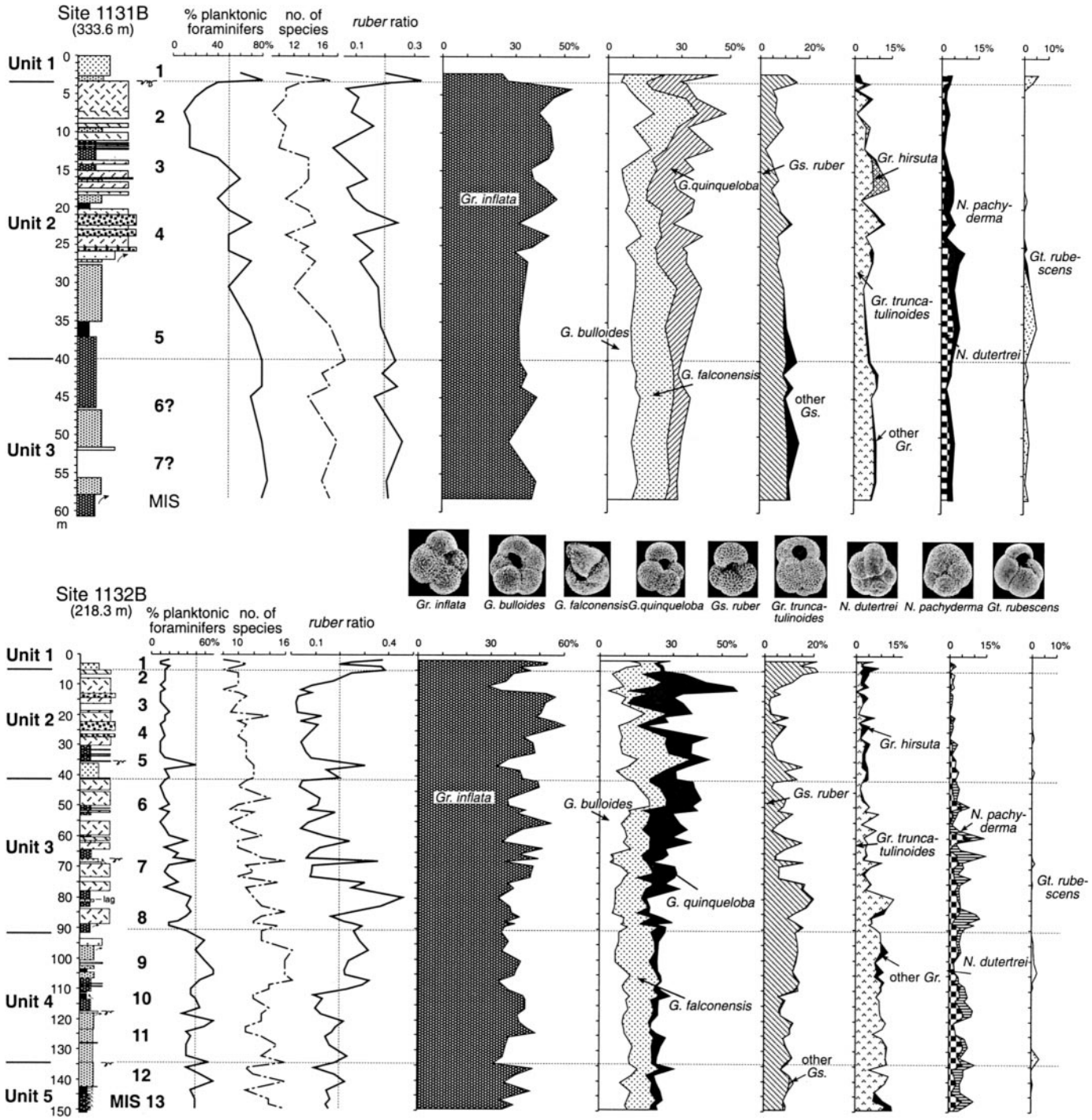

FIG. 8.—The relative proportions of planktonic foraminifers in the upper 160 m at Site 1132 and upper 60 m at Site 1131B (legend in Fig. 3).

silt substrate, and in areas of moderate sedimentation rate. Furthermore, *Celleporaria* grow best in settings such as the GAB that are typically mesotrophic and particularly when oceanographic or climatic conditions lead to elevated nutrient levels in overlying surface waters (S.J. Hageman, personal communication 2002). Thus, mound growth, (i.e. the floatstones with a diverse FFEND assemblage) grew in paleowater depths no shallower than 120 m, with abundances in different floatstones indicating growth as deep as 250 m.

Nodular–arborescent forms are the most susceptible of all bryozoans to abrasion (Smith and Nelson 1996), thus their abundance in the cores further attests to *in situ* growth. Delicate branching forms grow across the seafloor spectrum to depths exceeding 450 m (Bone and James 1993). The forms that are conspicuous by their absence (the fenestrate *Adeona*) or presence in extremely low numbers (vagrant and foliose forms) achieve their highest numbers in modern high-energy shallow to outer-shelf environments, generally $<$ 100 m. The absence of these types in the cores points to little offshelf transport of these larger forms and supports the notion that floatstone macrobryozoan skeletons are largely *in situ.*

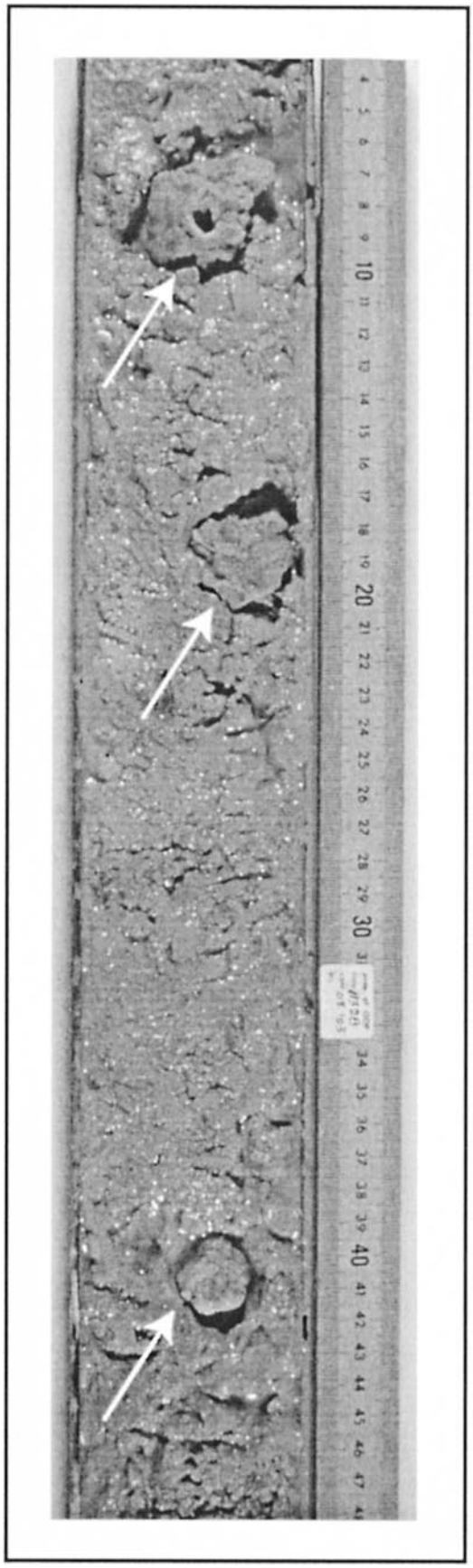

Shallow Versus Deep Mounds.—There are no dominant fenestrates in deep-water mounds (1131), whereas *Sertella* and *Triphyllozoon* are dominant in shallower buildups (1132, 1129). In contrast, while *Adeonellopsis* is a dominant flat robust branching form everywhere, in deep-water mounds (1131), *Bracebridgia, Caleschara, Labioporella,* and *Porina* are also abundant, i.e., the biota is more diverse. *Idmidronea* and *Nevianopora* always dominate the delicate branching skeletons together with *Hornera* in shallow water and *Tubulipora* in deeper mounds (Appendix 1, see Acknowledgments).

Younger Versus Older Mounds.—Although there are no significant differences between older (unit 3) and younger (unit 2) mounds, several subtle trends are evident (Appendix 1, see Acknowledgments). The youngest mounds have fewer dominant forms (i.e., fewer growth forms yield the same proportion of skeletons), and there are significantly higher numbers of fenestrates (but with lower diversity). These higher numbers of fenestrates likely reflect growth in shallower water.

In summary, mounds are composed of a macrofossil bryozoan biota that represents growth in an upper-slope environment (120–250 mwd) consisting of forms broadly similar to those on the upper slope today but in vastly greater numbers. The biota is generally similar both stratigraphically and spatially, with differences between shallow and deep, old and young mounds reflecting subtle variations within the FFEND assemblage.

Sediment Composition

Sediment throughout this entire upper slope-shelf margin setting is remarkably similar, consisting of bryozoan-dominated, foraminifer-rich, heterozoan, muddy carbonate, with only subtle differences between mound and inter-mound material. The composition of floatstone from seismic mound core and mound flank facies is not substantially different, indicating a similar biota across the surface of the mound. Bedded intermound sediment always contains sparse bryozoan fragments of varying grain size. Allochems are typically fragmented and generally somewhat abraded, commonly gray and biodegraded, with microbial borings. Although generally burrowed, they are also locally coarse-to-fine upward graded, implying redeposition. In contrast, mound floatstones are heterogeneous, with particles typically well preserved whole to angular fragments, implying biofragmentation, minimal transport, and relatively rapid, in-place accumulation.

Carbonate mud is mostly of silt size, with little clay-size material. The finest sizes are rich in coccolith debris, both whole discs and platelets, whereas coarser bioclasts are whole to fragmented-disarticulated, small, benthic skeletons and sponge chips. Floatstones are conspicuously richer in coccoliths than are bedded packstones. These phytoplankton remains may be from direct settling through the water column and/or from resedimentation of fine material from the shelf. Regardless, large numbers imply elevated trophic resources and higher water-column primary productivity.

Additional constituents include fecal pellets and terrigenous clastic grains. Fecal pellets of medium to coarse sand size, soft in units 1 to 3 but hard below ~ 90 mbsf, are too large for bryozoan feces (Best and Thorpe 1987; Winston 1977) but about right for crustaceans and worms and are commensurate with numerous burrow fabrics. Certain layers are rich (~ 20%) in fine to very fine quartz sand grains, but there is no direct correlation with eustasy. There is no local source of quartz, so it must either have been delivered by longshore drift from the west or, in the case of the fine fraction, be eolian.

One of the most perplexing compositional aspects of these sediments is the ubiquity of coralline algae pieces in both mound and intermound sediment. There is no clear trend, although they are slightly more numerous

←

FIG. 9.—Core 1132B-03H-3-20.33 to 20.83 cm (~ 22 mbsf; unit 2B) illustrating large *Celleporaria* sp. bryozoan colonies (arrows) in floatstone.

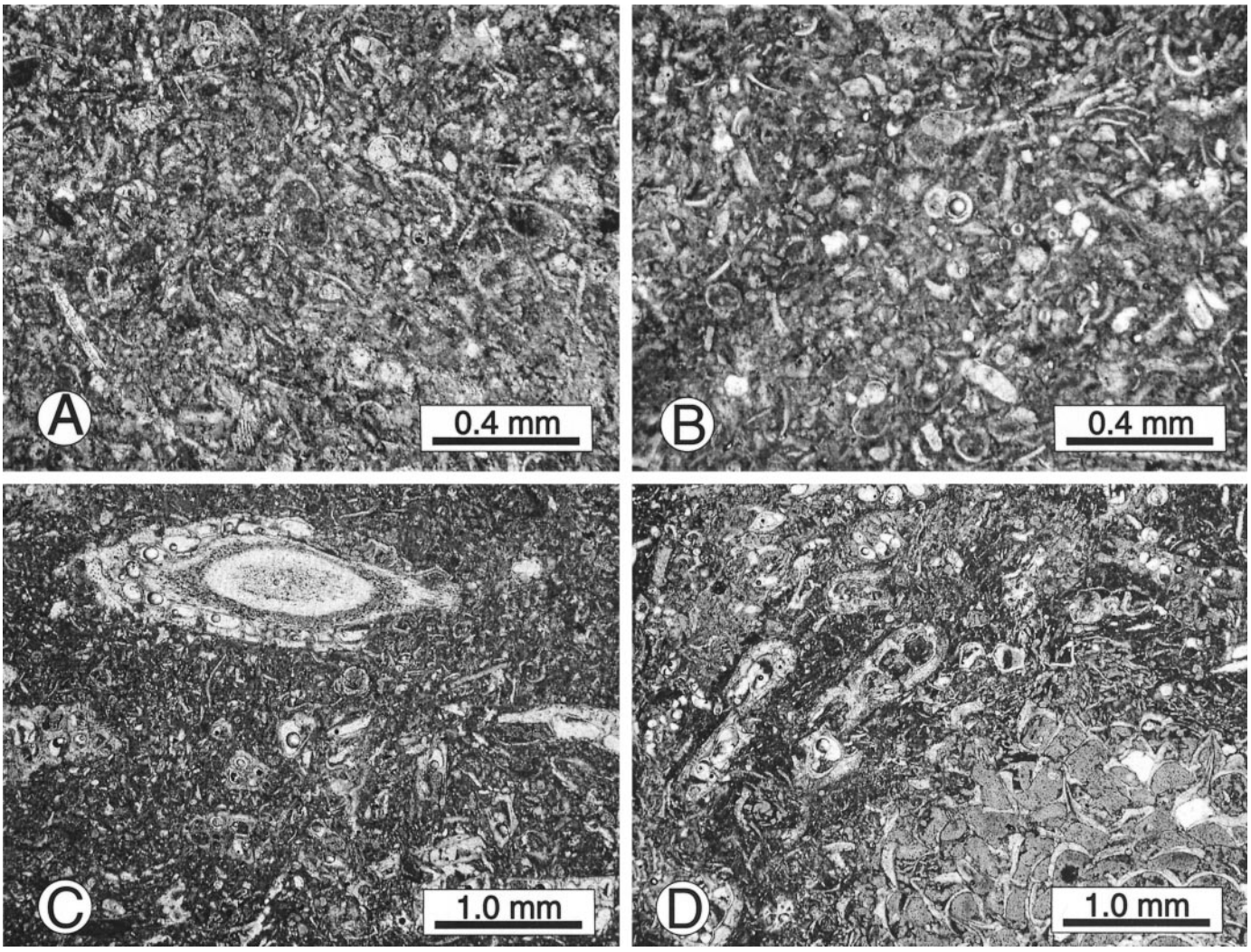

FIG. 10.—Photomicrographs, plane-polarized light. **A)** Muddy packstone replete with numerous small curved shells of ostracods and foraminifer fragments, 1129-17H-3-22 cm, 153.02 mbsf, unit 5. **B)** Muddy packstone with numerous planktonic foraminifers, 1129-13H-6-64 cm, 119.64 mbsf, unit 4A. **C)** Sparse bryozoan floatstone with bryozoan-bioclast packstone matrix, 1129-5H-51-56 cm, 42.31 mbsf, unit 3B2. **D)** Rich bryozoan floatstone with numerous coarse skeletal fragments and whole skeletons, mostly bryozoans, 1129-6H-5-50 cm, 51.8 mbsf, unit 3B2.

during lowstands and mound growth. Today the photic zone extends to ~ 110 mwd and living corallines occur to water depths of 60 m in the GAB (James et al. 2001). They are most prolific as articulated particles in grass beds, which grow best to ~ 30 mwd. Assuming that mounds were thriving at depths of ~ 120–240 mwd, this is far too deep for prolific coralline production. Given that the shelf was narrower during lowstands (James et al. 1997) and nutrient supply somewhat elevated, shallow-water coralline productivity was probably somewhat higher, and close to the shelf edge. The inevitable conclusion is that these particles are a clear signal of an offshelf, allochthonous contribution to the mound sediment. Further, they are a caution for the interpretation of algae particles in mounds in the rock record.

The Mound Growth Window

Paleodepth Limits.—The mound growth window can be framed with the preceding information, the depth of mound growth during the latest Pleistocene, the sea-level curve, and calculation of seafloor depths for older periods of growth (Table 4). The maximum fall in sea-level (e.g., MIS 2 and 6) of 120 m is used, reflecting both sea-level fall and isostatic compensation due to decreased water load during sea-level fall. Paleoseafloor depths are given by current water depth minus paleo sea level plus sediment thickness.

During the last phase of mound growth (MIS 2) bryozoans flourished between ~ 100 and ~ 260 mwd (deepest mound flank). The lower limit

→

FIG. 11.—SEM photomicrographs of fine-grained components. **A)** Sponge spicules in bryozoan floatstone; unit 2B; 12.88 mbsf,1132-2H-5-8 cm. **B)** Numerous coccoliths in matrix of grainy packstone; unit 2B, 12.44 mbsf, 1129-2H-4-64 cm. **C)** Ascidian spicule (arrow) in grainy packstone; unit 2B, 12.44 mbsf, 1129-2H-4-64 cm. **D)** Small calcite crystals in matrix of Bryozoan floatstone, unit 3B3, 51.80 mbsf, 1129-6H-5-50 cm. **E)** Coarse-sand-size spicules, bryozoan fragments, and abraded particles in grainy packstone, unit 2B, 12.44 mbsf, 1129-2H-4-64 cm. **F)** Sponge spicules (arrow) and bryozoans in muddy packstone, unit2B2, 14.5 mbsf, 1131-2H-5-49 cm.

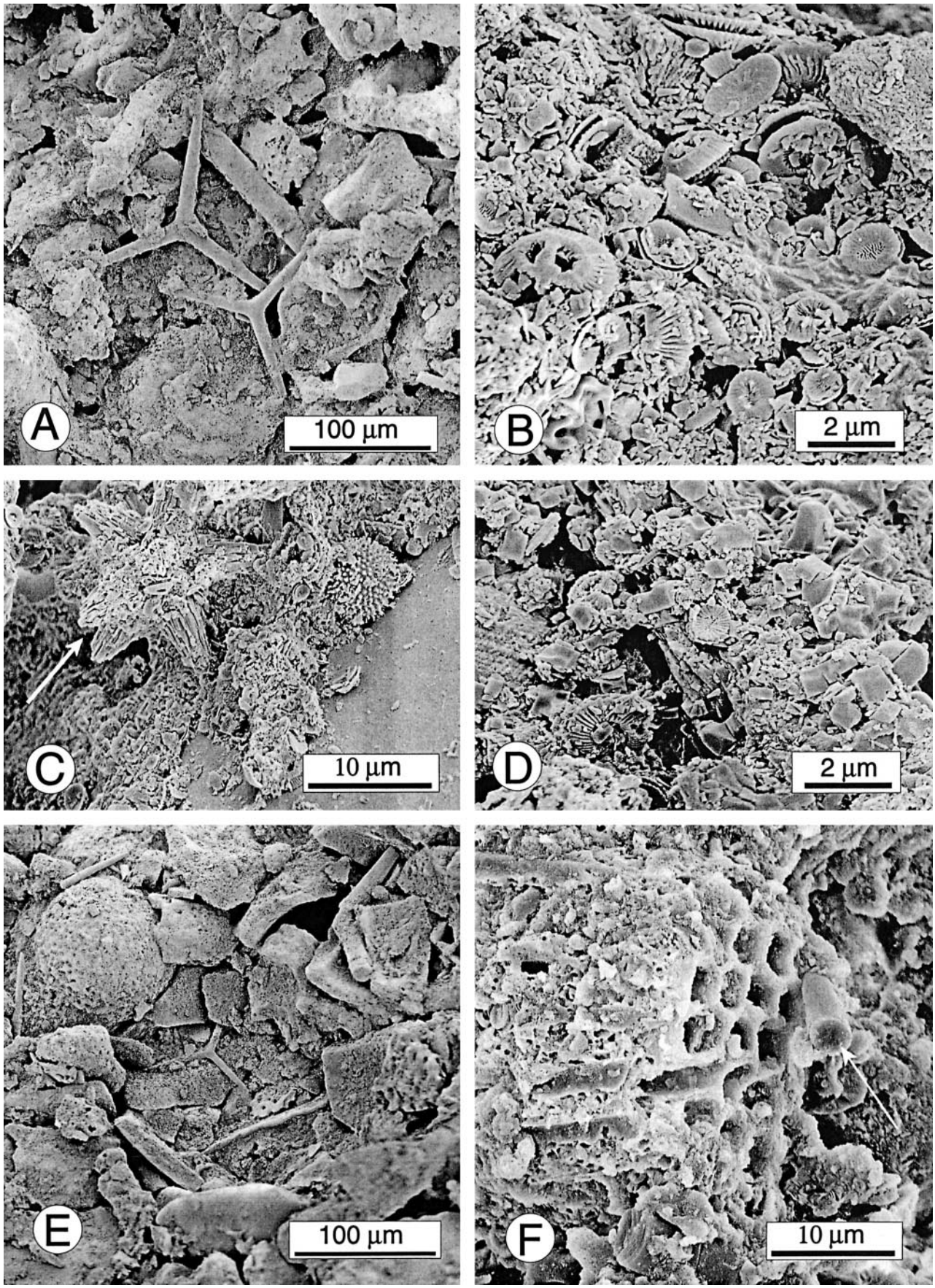
A
100 µm
B
2 µm
C
10 µm
D
2 µm
E
100 µm
F
10 µm

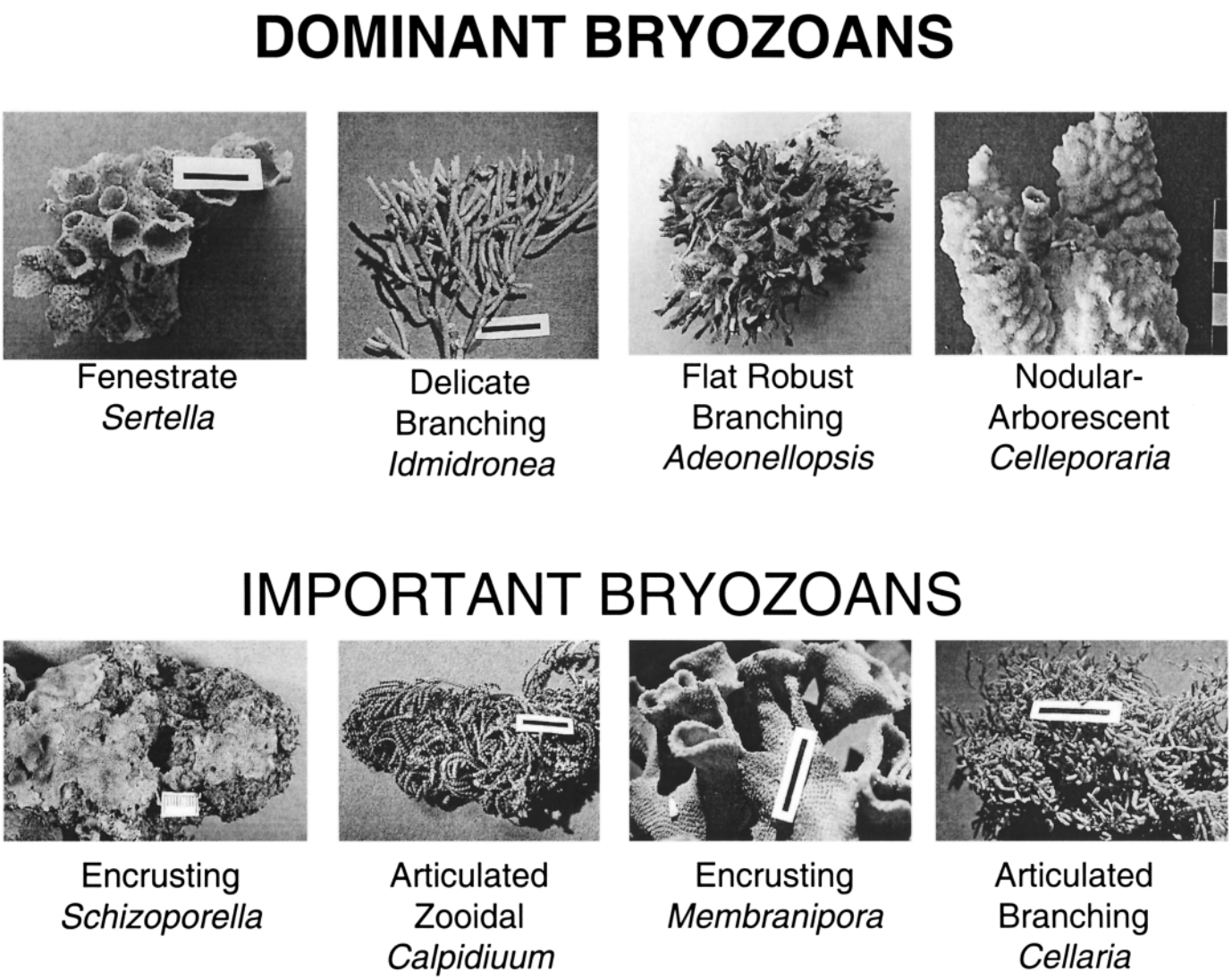

FIG. 12.—Photographs of living examples of some of the main bryozoans in the FFEND assemblage encountered in mound facies.

of growth appears to be consistent through time. At Site 1131 the paleo-water depth prior to MIS 5 was always > 260 m, and there was no mound growth. Mounds did not develop at Sites 1132 and 1129 prior to MIS 8, when the seafloor was deeper than ~ 220 mwd. Thus, the mound growth window lay between paleo-seafloor depths of ~ 100 and ~ 240 m. As noted previously this is compatible with depth distributions of the modern bryozoans in the FFEND assemblage.

The upper limit can be ascribed to swell wave base. The modern shelf is constantly swept by large, long-period swells that originate north of Antarctica (James et al. 2001), and as a result sediments in < 70 mwd are moved constantly. Reasons for the lower limits are less clear, although foraminiferal analyses provide a valuable perspective. The *B. marginata* benthic foraminiferal assemblage, indicative of mesotrophic conditions, as well as high numbers of large specimens (> 1 mm), typify MIS 1 to 8 (units 1 to 3) at shallow Sites 1132 and 1129 and MIS 1 to 4 (units 1 and 2) at the deeper Site 1131. In contrast the *P. wuellerstorfi* assemblage, with more oligotrophic forms, occurs in underlying MIS 9 to 12 (Sites 1132–1129) and MIS 5 and older (Site 1131) sediments. *P. wuellerstorfi* is generally used as an indicator of low to intermediate carbon flux for water depths greater than 1000 m (Altenbach et al. 1999). The *P. wuellerstorfi* assemblage contains other bathyl species that are usually absent from a shelf assemblage (*E. pacifica*, *G. orbicularis*, *C. auriculus*). Their presence suggests an extremely low carbon flux at the seafloor.

Planktonic foraminifers show a similar partitioning. Units 4 and 5 (MIS 9 to 13) contain not only more planktonic foraminifers (40–70%) but also abundant *G. truncatulinoides* (~ 10%). Together with the consistent occurrence of some warm-water species of *Globigerinoides* and *Globorotalia*, these biofacies features suggest mesotrophic to weak oligotrophic conditions during MIS 9 to 13. These foraminiferal results suggest that the lower limit of mound growth, at a calculated paleo-water depth of ~ 240 m (Sites 1132 and 1129) to 260 m (Site 1131) coincides with a change from a eutrophic to more mesotrophic (weak oligotrophic) watermass (Fig. 21).

Trophic Resources.—Bryozoans feed primarily on unarmored phytoplankton (McKinney and Jackson 1989), and consequently their growth

→

FIG. 13.—Lithostratigraphy of units 4 and 5 at Sites 1132 and 1129. Seismic facies are from Figures 5, 7. MIS = marine isotope stages.

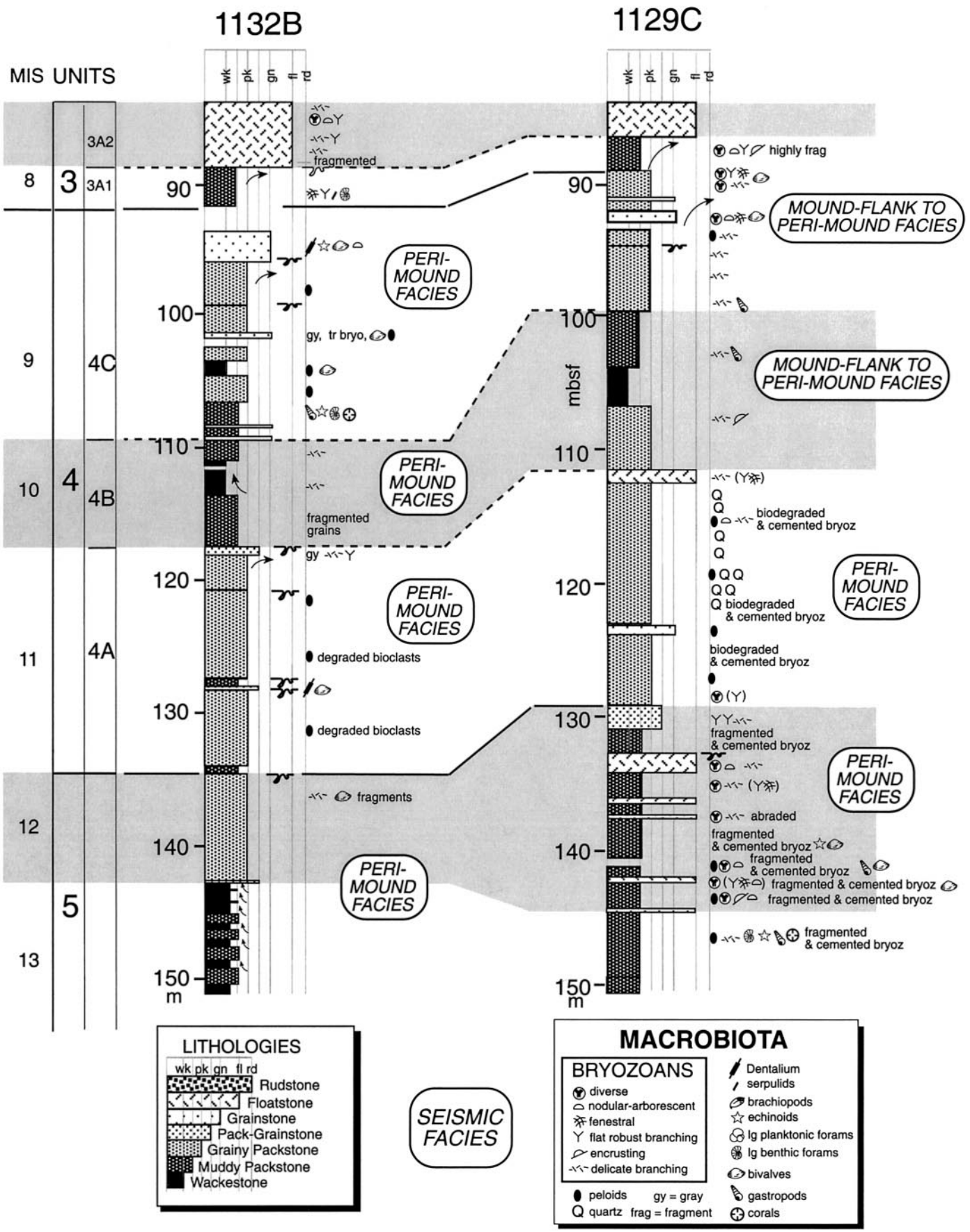
1132B
1129C
MIS UNITS
wk pk gn fl rd
3A2
3A1
4C
4B
4A
8
9
10
11
12
13
3
4
5
90
100
110
120
130
140
150
m
mbsf
fragmented
gy, tr bryo,
fragmented grains
gy
degraded bioclasts
degraded bioclasts
fragments
PERI-MOUND FACIES
PERI-MOUND FACIES
PERI-MOUND FACIES
PERI-MOUND FACIES
highly frag
MOUND-FLANK TO PERI-MOUND FACIES
MOUND-FLANK TO PERI-MOUND FACIES
biodegraded & cemented bryoz
biodegraded & cemented bryoz
biodegraded & cemented bryoz
fragmented & cemented bryoz
abraded
fragmented & cemented bryoz
fragmented & cemented bryoz
fragmented & cemented bryoz
fragmented & cemented bryoz
fragmented & cemented bryoz
LITHOLOGIES
wk pk gn fl rd
Rudstone
Floatstone
Grainstone
Pack-Grainstone
Grainy Packstone
Muddy Packstone
Wackestone
SEISMIC FACIES
MACROBIOTA
BRYOZOANS
diverse
nodular-arborescent
fenestral
flat robust branching
encrusting
delicate branching
peloids gy = gray
Q quartz frag = fragment
Dentalium
serpulids
brachiopods
echinoids
lg planktonic forams
lg benthic forams
bivalves
gastropods
corals

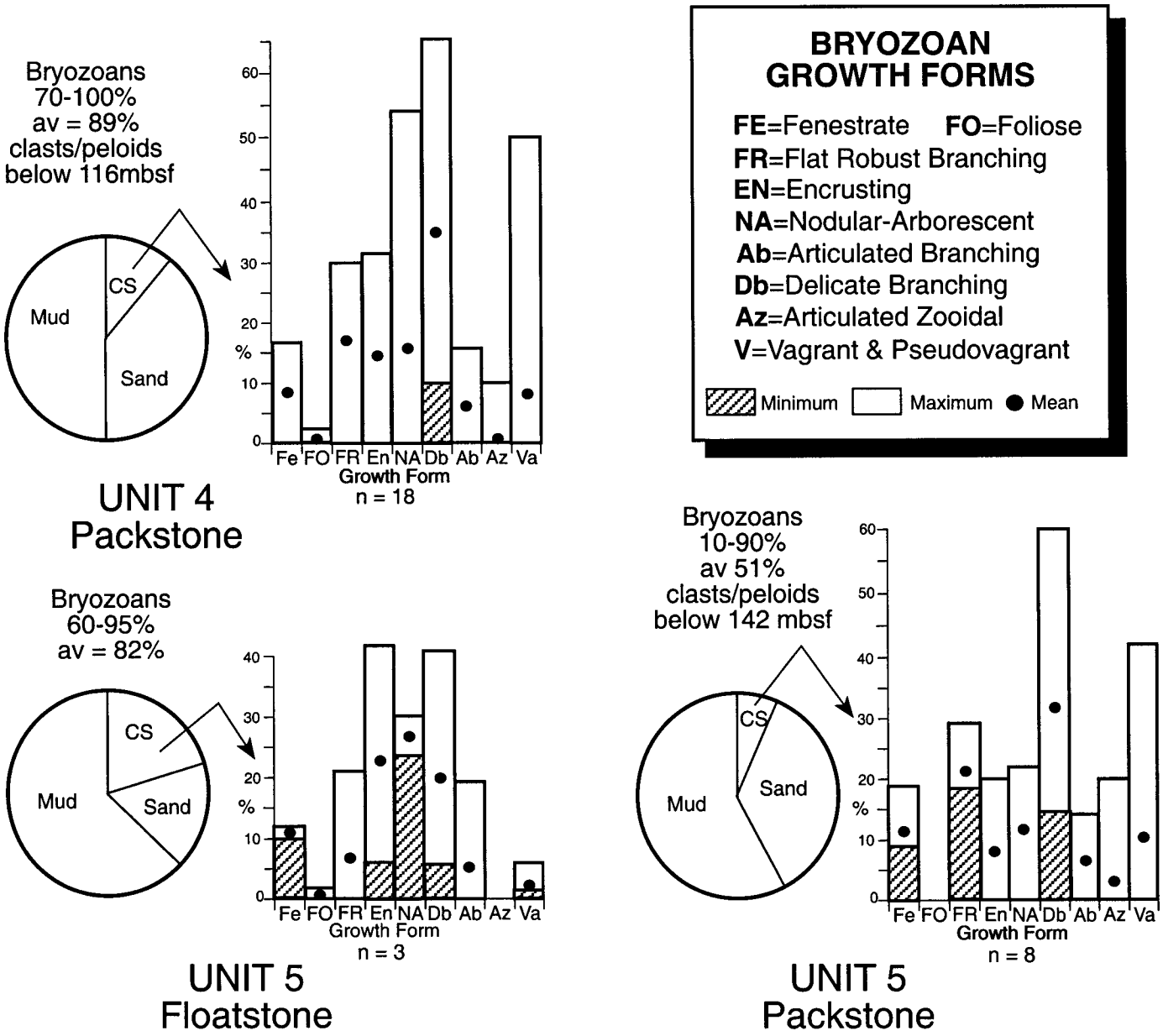

FIG. 14.—Relative proportions of bryozoans in different lithologies in units 4 and 5 from Site 1129.

and abundance is directly related to levels of primary productivity. GAB slope mounds are composed of a bryozoan community similar to that occurring in upper-slope environments today, implying that there was no major change in the biotic diversity between glacial and interglacial habitats, but rather a major increase in trophic resources and thus bryozoan abundance during glacial periods.

Benthic foraminifers further illustrate the link between lowstands and elevated trophic resources, with assemblages in mounds indicative of high carbon flux. This confirms both euphotic and high nutrient conditions during even-numbered MIS glacial periods (Holbourn et al. 2002). The same relationship is also true for planktonic foraminifers, where the correlation between mounds and high abundance of *G. inflata* and *G. quinqueloba* indicates cool, nutrient-rich conditions along the southern Australian margin during glacials or periods of sea-level lowstand. Conditions in the upper water column during interglacials were warm and nutrient-deficient but probably not completely oligotrophic because the temperate species *G. inflata* still predominated over the less diverse planktonic foraminifer faunal assemblages.

These water-column changes between glacial and interglacial periods must have been related to glacial atmospheric–oceanic interaction, which in turn raises questions as to paleoclimate and paleoceanographic settings of the mounds.

→

FIG. 15.—Lithostratigraphy of unit 3 at Sites 1132 and 1129. Seismic facies are from Figures 5, 7. MIS = marine isotope stages.

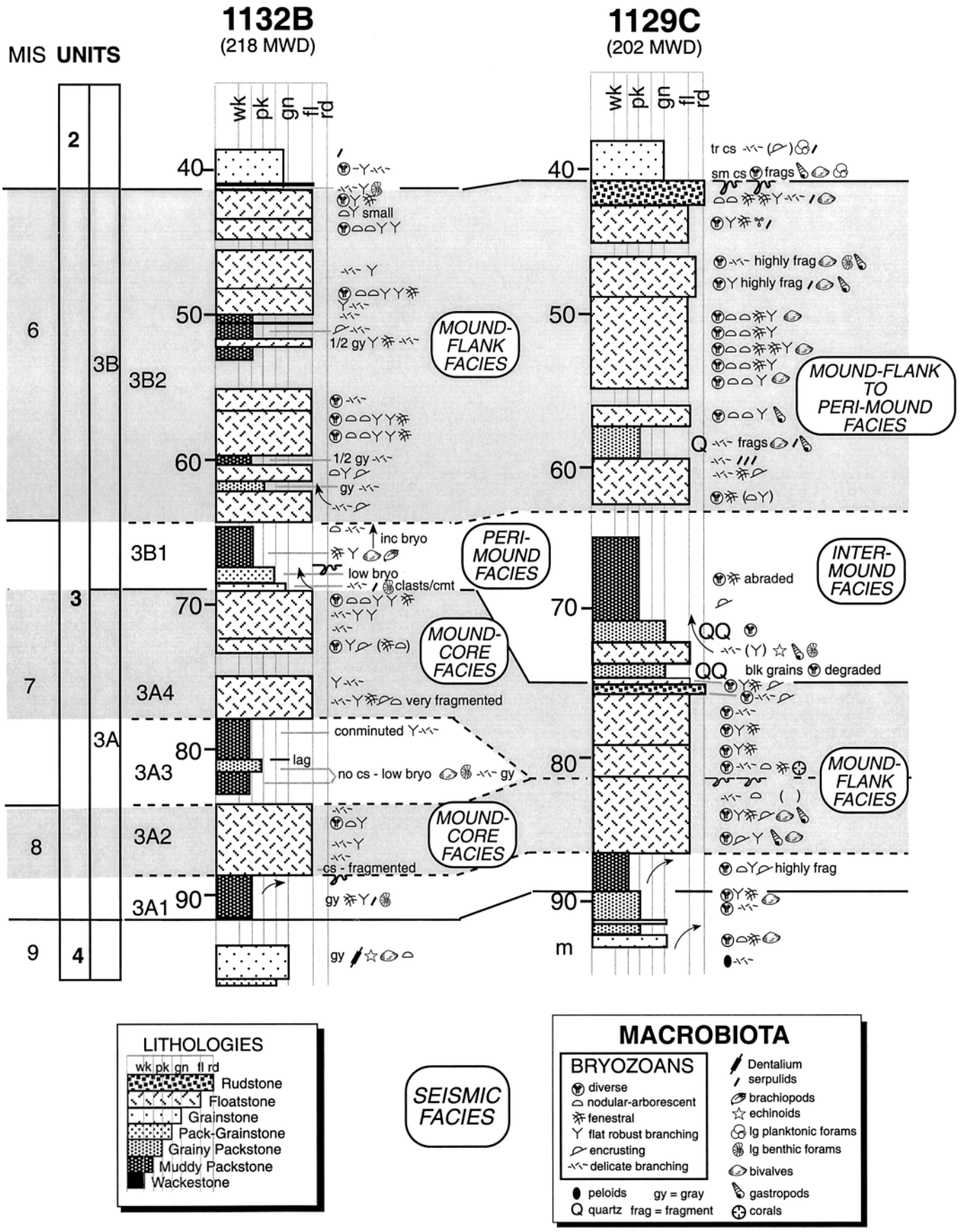
1132B
(218 MWD)
1129C
(202 MWD)
MIS UNITS
wk pk gn fl rd
40
50
60
70
80
90
m
2
3
4
6
7
8
9
3B
3A
3B2
3B1
3A4
3A3
3A2
3A1
small
1/2 gy
gy
inc bryo
low bryo
clasts/cmt
very fragmented
conminuted
lag
no cs - low bryo
cs - fragmented
tr cs
sm cs
frags
highly frag
abraded
blk grains
degraded
MOUND-FLANK FACIES
MOUND-FLANK TO PERI-MOUND FACIES
PERI-MOUND FACIES
INTER-MOUND FACIES
MOUND-CORE FACIES
LITHOLOGIES
Rudstone
Floatstone
Grainstone
Pack-Grainstone
Grainy Packstone
Muddy Packstone
Wackestone
SEISMIC FACIES
MACROBIOTA
BRYOZOANS
diverse
nodular-arborescent
fenestral
flat robust branching
encrusting
delicate branching
Dentalium
serpulids
brachiopods
echinoids
lg planktonic forams
lg benthic forams
bivalves
gastropods
corals
peloids
quartz
gy = gray
frag = fragment

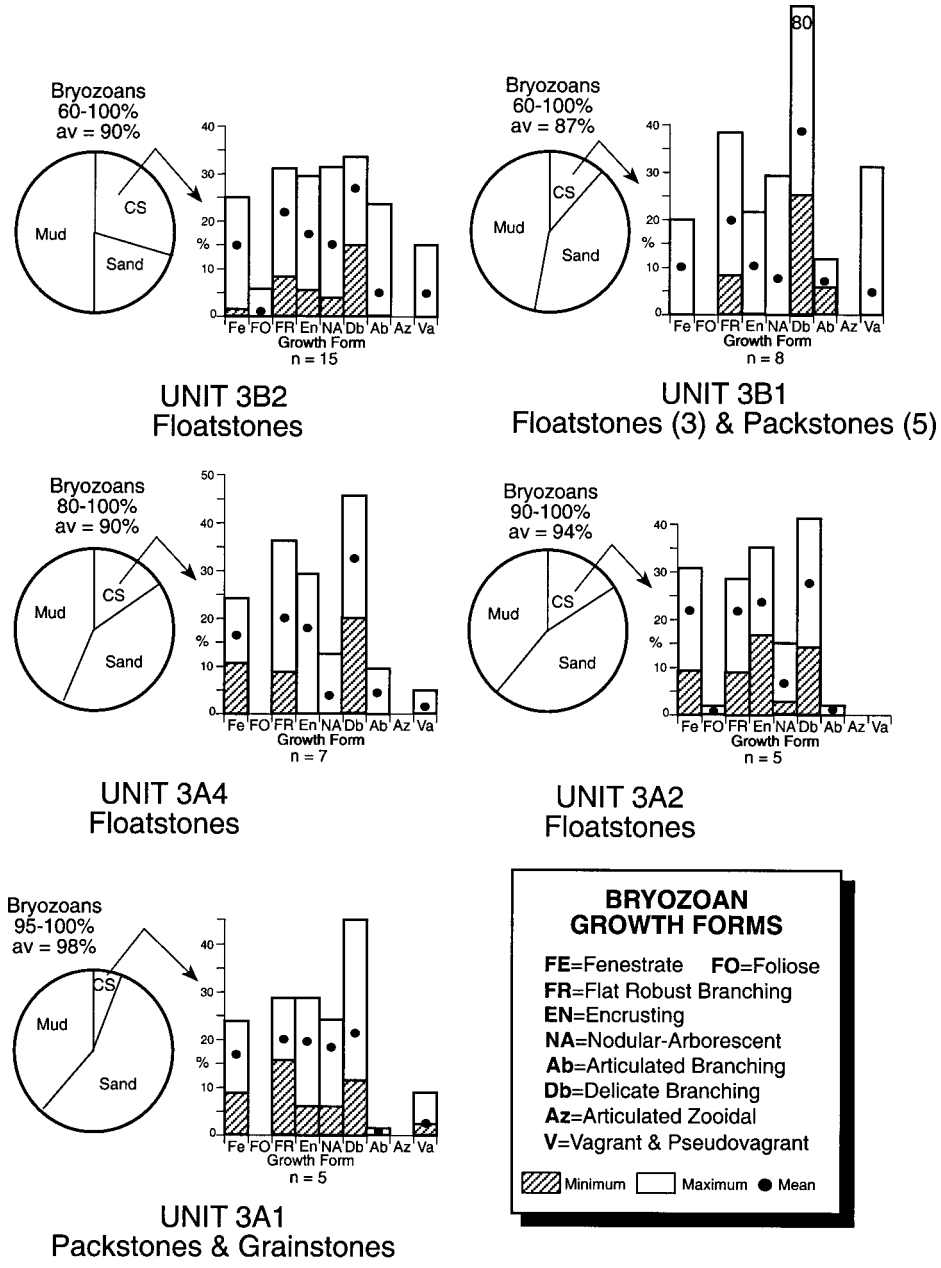

FIG. 16.—Relative proportions of bryozoans in different lithologies in unit 3 from Site 1129.

Paleoclimate.—There is a general consensus that in Pleistocene glacial periods continental Australia was cooler (~ 5–8°C) and much drier than today, with a stronger and larger high-pressure cell centered north of the GAB (Williams et al. 1998). Paleodune systems attest to strong westerlies across all of southern Australia (Jennings 1968; Sprigg 1978; Williams 2001). Consequently, storm systems and low-pressure cells would have been pushed well south of the continent.

The last glacial maximum (LGM) serves as an analog for all of the late Pleistocene lowstands when mounds flourished. Sea level was dramatically lower than present, so the GAB was then a wide coastal plain backed by paleo-seacliffs (Fig. 21). The geometry of the shoreline was largely latitude-parallel rather than the oceanic embayment present today. Most of the coastal plain would have been covered with quartzose dunes, which are today moribund structures largely covered with vegetation on the western Roe Plain. This quartzose sand is now mixed with Holocene carbonate on the present-day inner shelf and mid-shelf (James et al. 2001). Climate was somewhat more humid near the shoreline (cf. Williams 2001; winter rainfall > 250 mm), like the Nullarbor Plain today. Consequently, there was not massive offshore transport of terrigenous fines, because these were blown mostly to the east, not south. Furthermore, no rivers of any consequence drained into the central GAB. Thus, there was no fluvial input of nutrients during lowstand mound growth, although there may have been some eolian terrestrial nutrient flux via airborne dust.

Paleoceanography.—At present, the complex water masses on and adjacent to the GAB are bounded to the south by the global subtropical convergence zone separating subtropical and subantarctic surface water masses. Ranging between 35°S and 45°S, this wide band is where cold, low-salinity, nutrient-rich Antarctic Intermediate Water converges with and slides northward beneath relatively warm, high-salinity, oligotrophic Subtropical Central Water. This zone is characterized by steep thermal gradients (~ 10–15°C and strong downwelling. There is a global region of nutrient increase just north of the subtropical convergence zone and chlo-

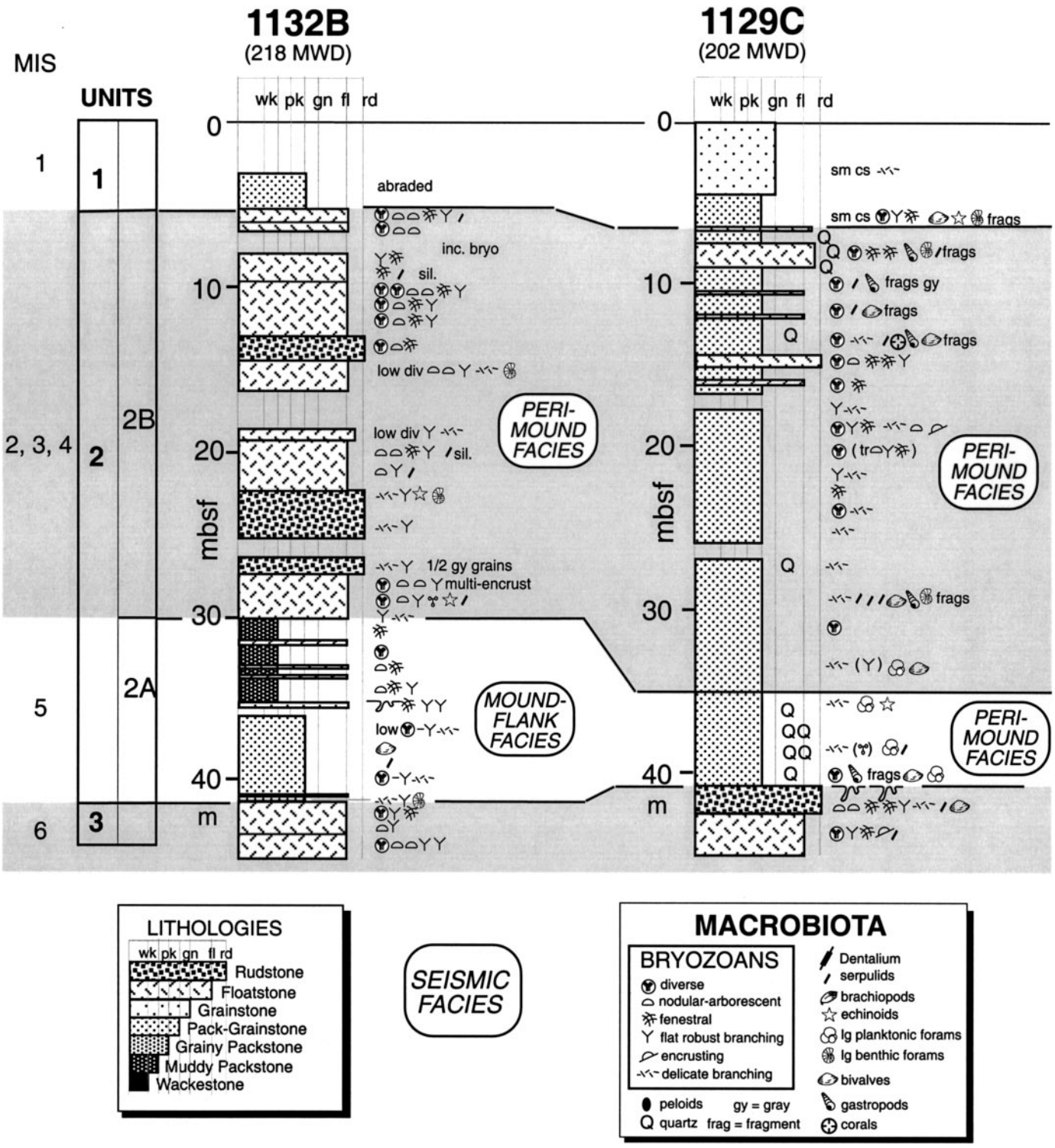

FIG. 17.—Lithostratigraphy of units 1 and 2 at Sites 1132 and 1129. Seismic facies are from Figures 5, 7. MIS = marine isotope stages.

rophyll enhancement, reflecting expanded primary productivity (Buttler et al. 1992; Clementson et al. 1998) best explained by a variety of mechanisms related to mixing (Longhurst 1998).

The modern shelf in the Eyre Terrace region is a region of overall downwelling (James et al. 2001), with any upwelling, especially during winter months, inhibited by the Leeuwin Current, a shallow, eastward-flowing current of nutrient-depleted water at the shelf edge (Herzfeld 1997).

The shelf was much narrower (estimated < 40 km wide) during glacial lowstands and there was no eastward-flowing Leeuwin Current along the shelf margin to prevent upwelling (Almond et al. 1993; Wells and Wells 1994; Wells et al. 1994; Okada and Wells 1997), leading James et al. (2000) to propose enhanced upwelling as the cause of mound growth. While this may be in part true, the situation now appears more complicated. First, $\delta^{18}O$ records indicate higher temperatures at Site 1129 than at Site

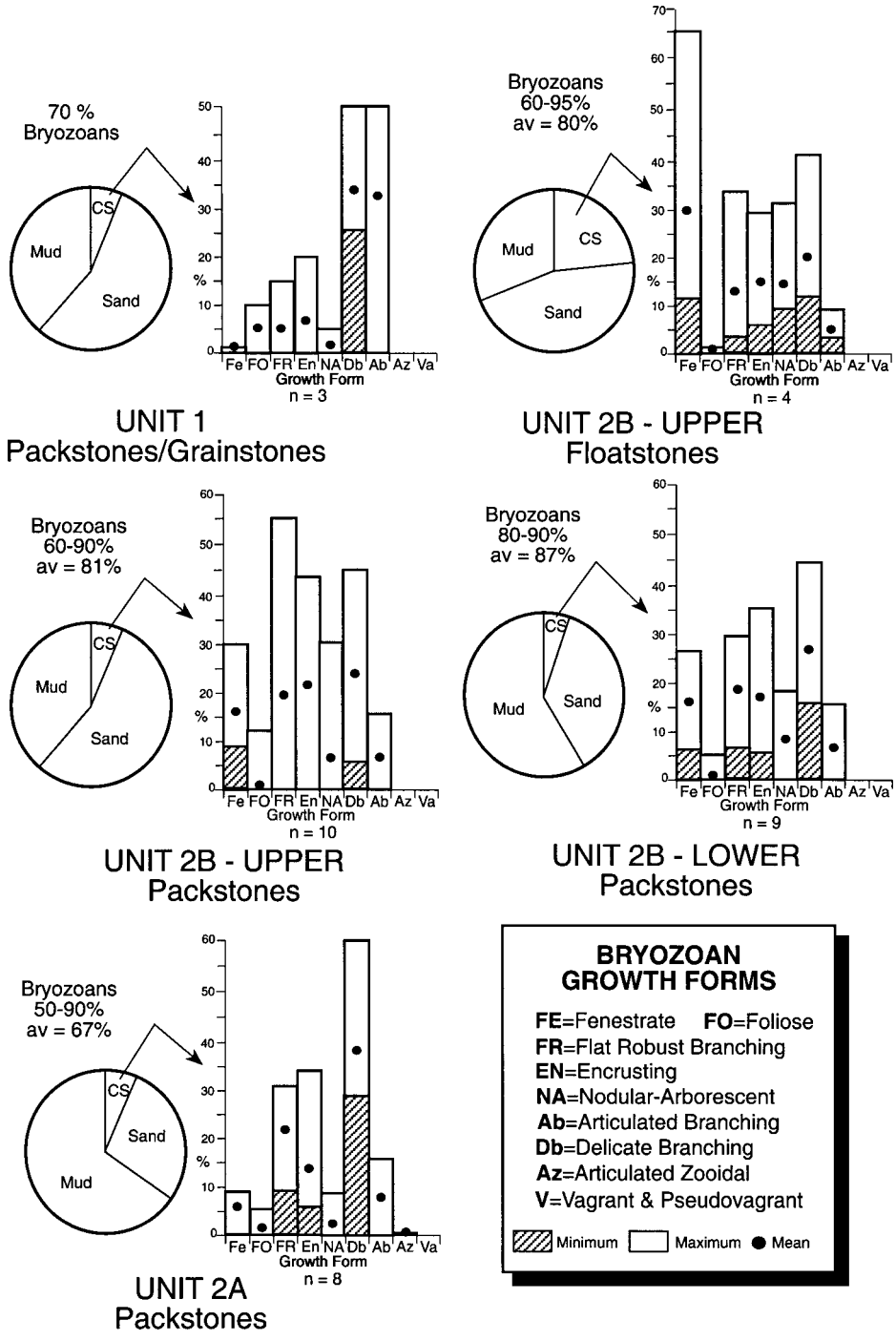

FIG. 18.—Relative proportions of bryozoans in different lithologies in units 1 and 2 from Site 1129.

1132 in MIS 2 to 4 (Fig. 7) (Holbourn et al. 2002), implying that local conditions varied greatly as they do today (James et al. 2001). Second, with an enlarged high-pressure cell and attendant anticyclonic circulation, the whole area would have been subject to strong westerlies and coastal downwelling. Upwelling would have occurred only if the high-pressure cells moved south of the shelf. Third, the foraminiferal record from this study indicates a largely oligotrophic water mass lying at a paleodepth of generally greater than 250 mwd, with mounds growing in nutrient-enriched waters above it, a situation incompatible with upwelling. This implies a much different offshore paleoceanography during lowstands and mound growth.

Sea-surface temperatures during the LGM are estimated to have been 16–12°C at the GAB shoreline (summer–winter) and 12–10 C at the shelf edge, roughly 3–5° C less than they are today (Barrows et al. 1996; Barrows et al. 2000). This would essentially have been the Subantarctic Zone, as indicated by slope cores to the east (Lynch-Steiglitz et al. 1994). The Subtropical Convergence Zone seems to have been equatorward of its modern position for much of the last 500 ky (Howard and Prell 1992), and during glacial periods is estimated to have moved 2° to 5° north of its present location (Prell et al. 1979; Prell et al. 1980). The consensus seems to be that it was never much farther north than 35°S, which is still close to the GAB shelf edge at ~ 33.5–34°S (< 120–180 km). Finally, it appears that

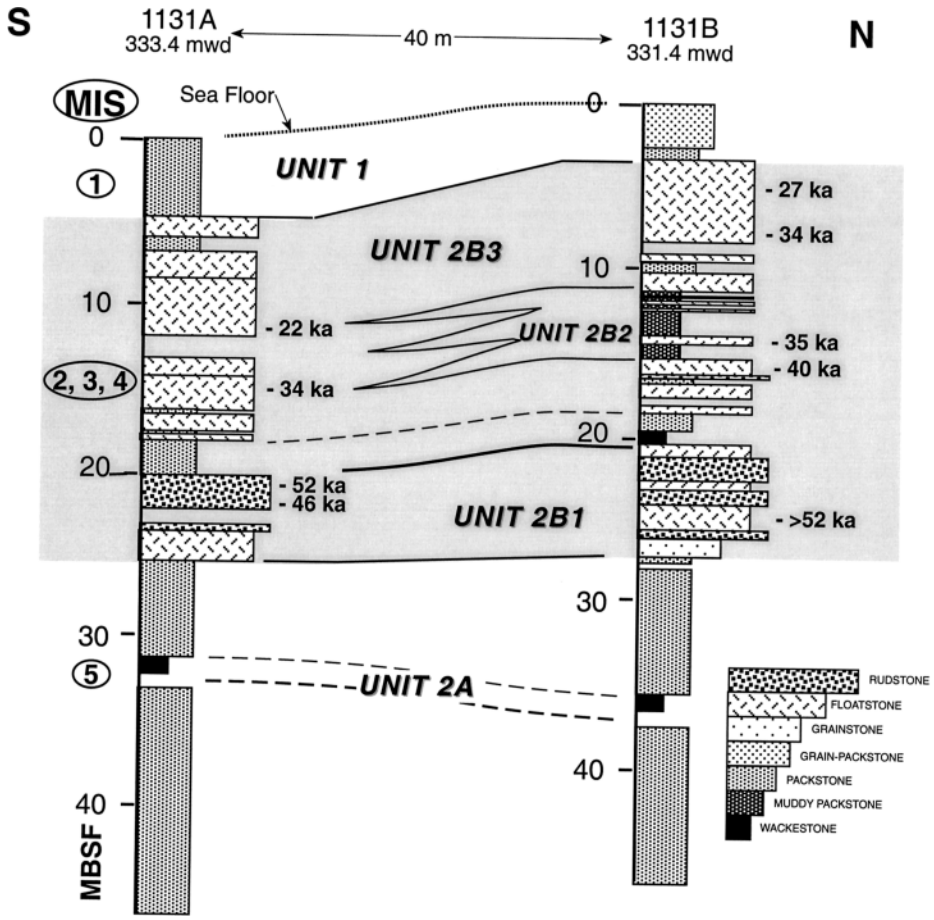

FIG. 19.—Lithostratigraphy and correlation of units 1 and 2 from Sites 1131A and 1131B. Seismic facies are from Figure 6. MIS = marine isotope stages.

during glacial periods the Southern Ocean overall was an area of nutrient enhancement (Nelson et al. 1993; Ikehara et al. 2000), due, amongst other things, to an increase in Fe-rich atmospheric dust.

The most parsimonious explanation at present (Fig. 21) is that, whereas upwelling may have been important, the increased phytoplankton flux necessary for enhanced bryozoan, and thus mound growth, resulted from an overall nutrient increase in Southern Ocean water, together with northward movement of the Subtropical Convergence Zone and its region of elevated primary productivity to a position at or adjacent to the paleo-GAB shelf edge–upper slope.

Mound Succession

Distillation of sediment packaging in this late Pleistocene strata reveals a depositional pattern within the mounds that can be related to eustasy and paleoceanography (Fig. 22). Each mound comprises a series of phases 5–10 m thick.

Pre-Mound Phase.—Packstones and local grainstones are composed of numerous allochthonous particles. The sediment contains progressively more whole, abraded, bryozoan biofragments upward.

Mound Phase.—Basal mound sediment is floatstone rich in delicate branching, commonly fragmented bryozoans indicative of maximum water depth. Floatstones upward are marked by an increase in the number and diversity of bryozoans and reflect shallowing. They reach a maximum in the middle and upper parts of the mound. Skeletons are generally whole and best preserved here. Upper lithologies tend to be dominated by bryozoan-rich floatstone and rudstone. These middle and upper mound sediments can be punctuated by erosion or omission surfaces. Uppermost sediments tend to be dominated by one or two bryozoan growth forms, usually delicate branching and fenestrate/flat robust branching types; fragmented skeletons are prominent locally.

Post-Mound Phase.—The top of the mound unit is either a sharp erosional surface or conspicuous firmground, directly overlain by packstone rich in biodegraded, gray allochthonous grains. These overlying sediments contain relatively few bryozoans but numerous epifaunal bivalves, echinoids, serpulids, and locally large planktonic foraminifers.

These packstones grade upward into inter-mound sediments. Although highly variable, they become progressively muddier upsection, and are finest grained, locally with a lag, in the middle of the intermound interval. They contain allochthonous particles and were formed by downslope transport processes.

Thus, the mound and enclosing sediments are a recurring succession of predictable lithologies. Whereas sea level is the driving force, it is the attendant changes in oceanography that control the nature of sedimentation. Falling sea level and accompanying increased trophic resources result in nucleation and initial growth; most accretion takes place during lowstand; growth is abruptly terminated as conditions for growth are switched off by rapid sea-level rise, Leeuwin Current appearance, and oligotrophy during late sea-level rise and highstand, and the mound ''gives up.''

SUMMARY AND CONCLUSIONS

1. Upper-slope environments on the prograding carbonate wedge in the central GAB were sites of growth of bryozoan biogenic mounds throughout Pliocene–Pleistocene time. Regional seismic data show that these bryozoan floatstone-dominated mounds, the first such structures drilled in the modern ocean, grew in this environment over a distance of hundreds of kilometers across the central and western GAB.

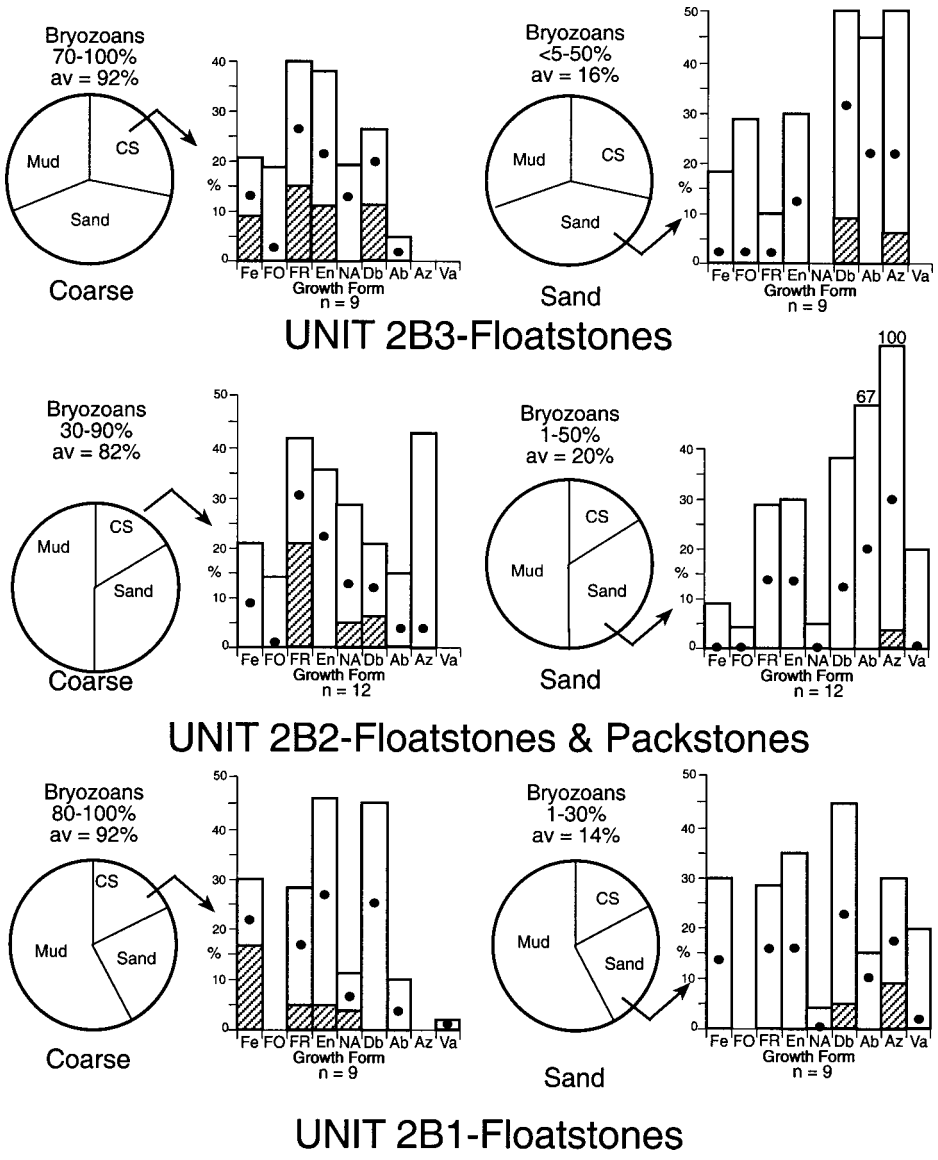

FIG. 20.—Relative proportions of bryozoans in different lithologies in units 1 and 2 from Site 1131B.

TABLE 4.—*Paleo-seafloor depths.*

MIS	Units	Relative Sealevel	Sea Level (meters below present)	Sediment Thickness (m)	Paleo-seafloor Depth 1129 (202 mwd)	1132 (218 mwd)	1131 (334 mwd)
1	1	highstand	0	0	202	218	334
2	2B	lowstand	120	10	92*	108*	224*
3	2B	highstand	40	15	177*	193*	309*
4	2B	lowstand	90	20	132*	148*	264*
5	2A	highstand	0	35	237	253	369
6	3B2	lowstand	120	50	132*	148*	264*
7	3B1	highstand	0	65	267	283	399
8	3A	lowstand	90	80	192*	208*	324*
9	4B	highstand	0	100	302	318	434
10	4A	lowstand	80	120	242	258	374
11	4A	highstand	0	130	332	348	464
12	5	lowstand	120	140	222	238	354
13	5	highstand	0	150	352	368	484

MIS = Marine Isotope Stage. mwd = meters water depth.
* mound growth in study area.

2. Mounds are elongate, slope-parallel structures with paleorelief of up to 65 m and along-slope extents of as much as 2 km. Although present as widely distributed isolated mounds and smaller mound complexes since the Pliocene, mound growth seems to have been most active during latest Pleistocene time, resulting in extensive and thick mound complexes immediately below the modern shelf edge.

3. Unlithified burrowed mound floatstone contains 96 bryozoan genera, predominantly fenestrate, flat robust branching, encrusting, nodular–arborescent, and delicate branching growth forms (called herein the FFEND Assemblage). Although composed of roughly equal amounts of all forms, encrusting types are the most diverse whereas delicate branching forms produce the largest number of particles, albeit small. These bryozoans now grow in 100 to 250 mwd on the modern south Australian shelf. Facies differentiation is not strong, and the bryozoans likely flourished across the tops and along the flanks of the mounds.

4. Mounds are a combination of large *in situ* bryozoans, carbonate sand and mud from in-place production, off-shelf transport of mud, and planktonic fallout. It is primarily the in-place bryozoan growth and attendant biota that allowed the mounds to form positive relief. These buildups further acted as sources of carbonate sediment for the downslope wedge. Most

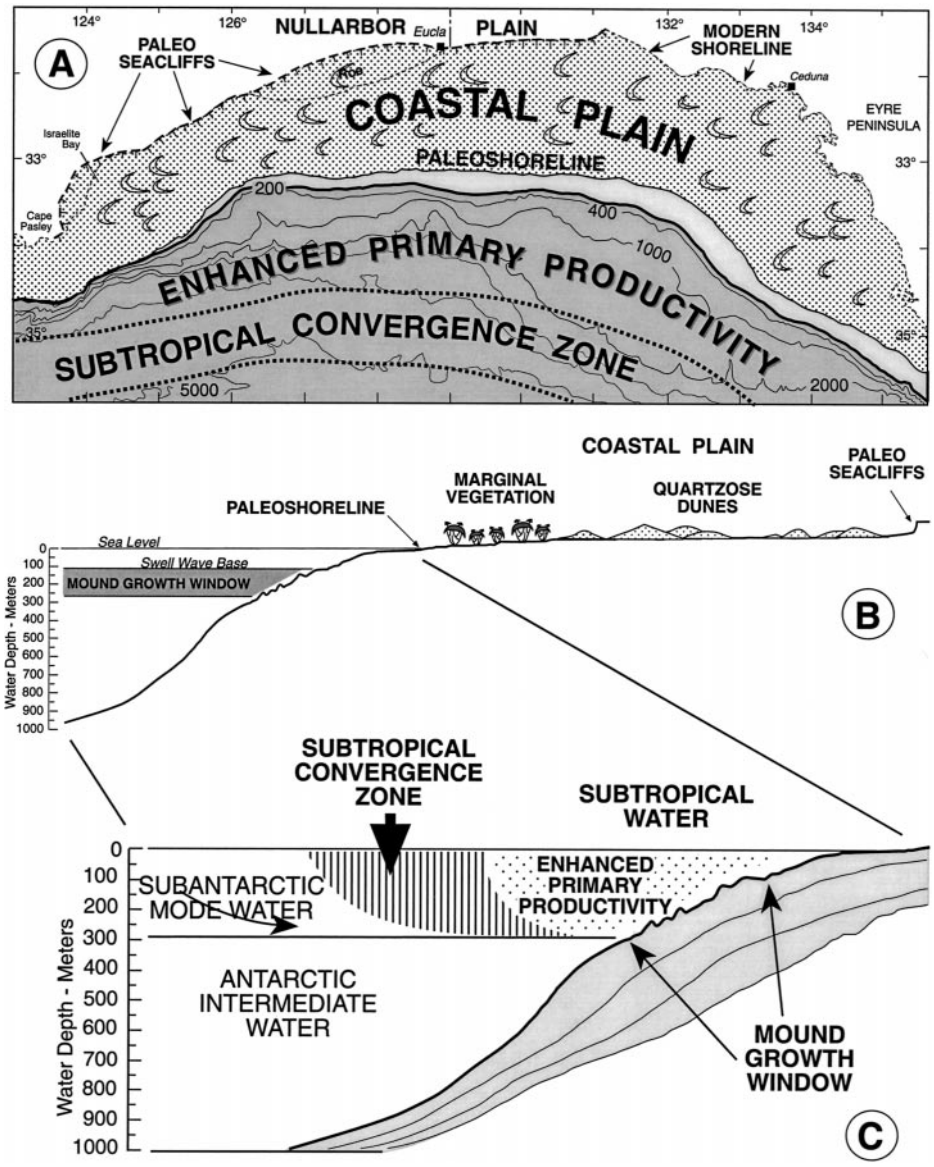

FIG. 21.—An interpretive sketch of conditions during glacial lowstands. **A)** Paleogeography, illustrating the wide coastal plain, narrow shelf, possible location of STCZ, and associated zone of enhanced primary productivity. **B)** A cross section of the coastal plain, shelf, and upper slope, illustrating location of the mound growth window. **C)** Enlarged view of shelf showing the interpreted paleoceanography and the probable location of major water masses.

of the fine-grained sand is made up of bryozoans, planktonic and benthic foraminifers, serpulids, coralline algae, sponge spicules, and peloids, with variable fine glauconite and quartz grains. Mud is rich in ostracods, tunicate spicules, bioeroded sponge chips, and coccoliths.

5. Radiometric dates and oxygen isotope stratigraphy indicate that mound growth took place principally during glacial lowstands (even-numbered MIS), while interglacial highstand sedimentation was mostly allochthonous carbonate and pelagic settling. Mound accretion was approximately vertical at rates of 30–67 cm/ky, while intermound, bedded sediment accumulated at rates of 17–25 cm/ky.

6. An integrated model of mound growth, comprising intervals 5–10 m in thickness, can be synthesized from the stacked buildups cored during Leg 182. Lowstand accumulation is interpreted to have begun with deposition of delicate branching bryozoan floatstone, which changed into a richer and more diverse bryozoan community that persisted through the buildup, even though periodically interrupted by times of nondeposition and/or erosion represented by omission surfaces. The upper parts of mounds are floatstone typified by a reduced bryozoan density and diversity, and numerous abraded grains that terminate abruptly or are capped by firmgrounds. Overlying highstand intermound sediments are generally packstones composed of fragmented, gray and bioeroded particles.

7. Mound growth is interpreted to have been a response to increased nutrient supply both on a regional and local scale during glacial periods. Enhanced trophic resources were likely the result of northward movement of the subtropical convergence and possible local upwelling. The window of mound growth, ~ 100 to 240 mwd, is thought to have been framed by the upper boundary of nutrient-poor, Antarctic Intermediate Water at the base and the lower limit of wave abrasion at the top.

ACKNOWLEDGMENTS

We thank Schlumberger officers, crew, and drillers and the Ocean Drilling Program laboratory personnel on Leg 182 and at College Station, Texas, for assistance throughout. Subsequent research was supported by the Natural Sciences and Engineering Research Council of Canada (NPJ), the National Science Foundation (JAS), the Australian Research Council (YB, QL), the Deutsche Forschungsgemeinschaft (AH, CB) and the Danish Natural Science Research Council (FS). Geochemical age dating was overseen by H. Schwarcz (McMaster University), P.M. Grootes and H. Erlenkeuser (Leibniz Laboratory, Christian-Albrechts University) and R.P. Beukens

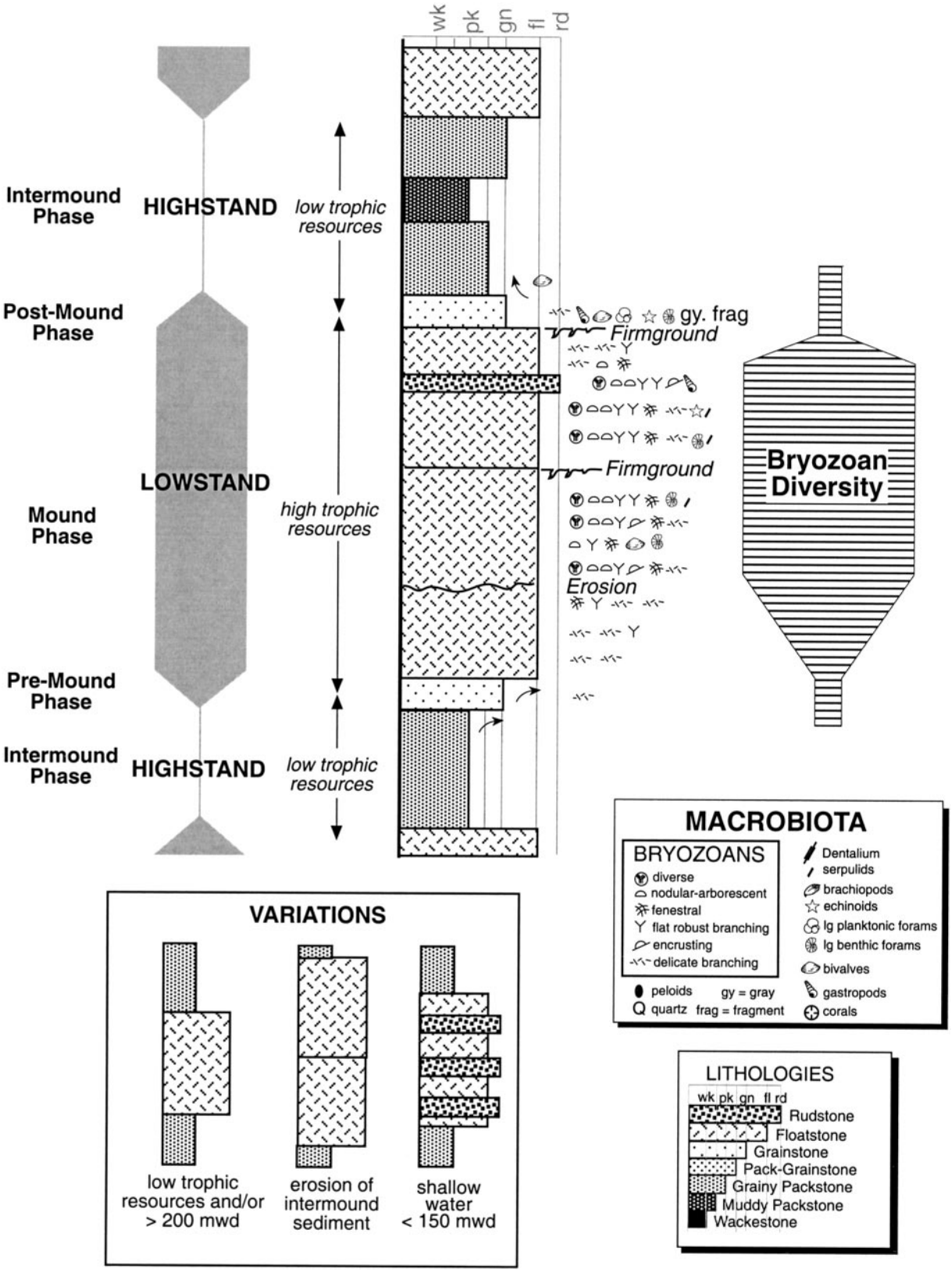

FIG. 22.—A sketch illustrating the interpreted typical bryozoan mound growth during a cycle from interglacial highstand to interglacial lowstand, based on results from this study. Expected variations are illustrated at base. Legend is in Figure 3.

(Isotrace, University of Toronto). SEM images were obtained with the help of G. Braybrook, University of Alberta. C. Koebernick assisted with manuscript preparation.

The data described in this paper have been archived, and are available in digital form, at the World data Center for Marine Geology and Geophysics, NOAA/NGDC, 325 Broadway, Boulder, CO 80303 (phone 303-497-6339); E-mail: wdcamgg@ngdc.noaa.gov; URL: http://www.ngdc.noaa.gov/mgg/sepm/archive/index.html.

REFERENCES

Almond, D.O., McGowran, B., and Li, Q., 1993, Late Quaternary foraminiferal record from the Great Australian Bight and its environmental significance, *in* Jell P.A., ed., Paleontological Studies in Honour of Ken Campbell: Association of Australian Paleontologists, Memoir 15, p. 417–428.

Altenbach, A.V., Pflaumann, U., Schiebel, R., Thies, A., Timm, S., and Trauth, M., 1999, Scaling percentages and distribution patterns of benthic foraminifera with flux rates of organic carbon: Journal of Foraminiferal Research, v. 29, p. 173–185.

Bard, E., Hamelin, B., Fairbanks, R.G., and Zindler, A., 1990, Calibration of the ^{14}C timescale over the past 30,000 years using mass spectronomic U–Th ages from Barbados corals: Science, v. 345, p. 405–410.

Barrows, T.T., Ayress, M.A., and Hunt, G.R., 1996, A reconstruction of the last glacial maximum sea-surface temperatures in the Australasian region: Quaternary Australasia, v. 14, p. 27–31.

Barrows, T.T., Juggins, S., De Deckker, P., Theide, J., and Martinez, J.I., 2000, Sea-surface temperature of the southwest Pacific Ocean during the Last Glacial Maximum: Paleoceanography, v. 15, p. 95–109.

Best, M.A., and Thorpe, J.P., 1987, Bryozoan faecal pellets: parameters and production rates, *in* Ross, J.R.P., ed., Bryozoa: Present and Past: Bellingham, Washington, Western Washington University Press, p. 17–24.

Bone, Y., and James, N.P., 1993, Bryozoans as carbonate sediment producers on the cool-water Lacepede Shelf, southern Australia: Sedimentary Geology, v. 86, p. 247–271.

Bone, Y., and James, N.P., 2002, Bryozoans from deep-water reef mounds: Great Australian Bight, Australia, *in* Wyse, J., Jackson, J.B.C., Buttler, R., and Spencer Jones, M., eds., Bryozoans 2001: Lisse, The Netherlands, Balkner Press, p. 9–14.

Boreen, T.D., and James, N.P., 1993, Holocene sediment dynamics on a cool-water carbonate shelf: Otway, southeastern Australia: Journal of Sedimentary Petrology, v. 63, p. 574–588.

Buttler, E.C.V., Butt, J.A., Lindsrom, E.J., Tildesley, P.C., Pickmere, S., and Vincent, W.F., 1992, Oceanography of the subtropical convergence zone around southern New Zealand: New Zealand Journal of Marine and Freshwater Research, v. 26, p. 131–154.

Clementson, L.A., Parslow, J.S., Griffiths, F.B., Lyne, V.D., Mackey, D.J., Harris, G.P., McKenzie, D.C., Bonham, P.I., Rathbone, C.A., and Rintoul, S., 1998, Controls on phytoplankton production in the Australasian sector of the subtropical convergence: Deep-Sea Research 1, v. 45, p. 1627–1661.

Dunham, R.J., 1962, Classification of carbonate rocks according to their depositional texture, *in* Ham, W.E., ed., Classification of Carbonate Rocks: American Association of Petroleum Geologists, Memoir 1, p. 108–121.

Embry, A.F., and Klovan, J.E., 1971, A Late Devonian reef tract on northeastern Banks Island, N.W.T.: Bulletin of Canadian Petroleum Geology, v. 19, p. 730–781.

Feary, D.A., 1997, ODP pollution safety panel Leg 182 safety package—Cenozoic cool-water carbonates of the Great Australian Bight: Australian Geological Survey, Organization Record 1997/28, 208 p.

Feary, D.A., and James, N.P., 1995, Cenozoic biogenic mounds and buried Miocene (?) barrier reef on a predominately cool-water carbonate continental margin—Eucla Basin, western Great Australian Bight: Geology, v. 23, p. 427–431.

Feary, D.A., and James, N.P., 1998, Seismic stratigraphy and geological evolution of the Cenozoic, cool-water Eucla Platform, Great Australian Bight: American Association of Petroleum Geologists, Bulletin, v. 82, p. 792–816.

Feary, D.A., Hine, A.C., Malone, M.J., et al., 2000, Great Australian Bight: Cenozoic cool-water carbonates: Proceedings of the Ocean Drilling Program, Initial Reports, v. 182: College Station, Texas, 58 p.

Hageman, S.J., Bone, Y., McGowran, B., and James, N.P., 1996, Bryozoan species distributions on the cool-water Lacepede Shelf, southern Australia, *in* Gordon, D.P., Smith, A.M., and Grant-Mackie, J.A., eds., Bryozoans in Space and Time: 10th International Bryozoology Conference, Proceedings, Wellington, New Zealand, p. 109–116.

Hageman, S.J., Bone, Y., McGowran, B., and James, N.P., 1997, Bryozoan colonial growth-forms as paleoenvironmental indicators: evaluation of methodology: Palaios, v. 12, p. 405–419.

Hageman, S.J., James, N.P., and Bone, Y., 2000, Cool-water carbonate production from epizoic bryozoans on ephemeral substrates: Palaios, v. 15, p. 33–48.

Hemleben, C., Spindler, M., and Anderson, O.R., 1989, Modern Planktonic Foraminifera: Berlin, Springer-Verlag, 561 p.

Herzfeld, M., 1997, The annual cycle of sea surface temperature in the Great Australian Bight: Progress in Oceanography, v. 39, p. 1–27.

Holbourn, A., Khunt, W., and James, N.P., 2002, Late Pleistocene reef-mounds of the Great Australian Bight: Isotope stratigraphy and benthic foraminiferal record: Paleoceanography, v. 17, p. 1–14.

Howard, W.R., and Prell, W.L., 1992, Late Quaternary surface circulation of the southern Indian Ocean and its relationship to orbital variations: Paleoceanography, v. 7, p. 79–118.

Ikehara, M., Kawamura, K., Ohkouchi, N., Murayama, M., Nakamura, T., and Taira, A., 2000, Variation of terrestrial input and marine productivity in the Southern Ocean (48°S) during the last two deglaciations: Paleoceanography, v. 15, p. 170–180.

Imbrie, J., Hays, J.D., Martinsen, A., McIntyre, A., Mix, A.C., Morley, J.J., Pisias, N.G., Prell, W.L., and Schackleton, N.J., 1984, The orbital theory of Pleistocene climate: support from a revised chronology of the marine $\delta^{18}O$ record, *in* Begeret, A.L., ed., Milankovitch and Climate, Part 1: Norwell, Massachusetts, D. Riedel, p. 269–305.

James, N.P., 1997, The cool-water carbonate depositional realm, *in* James, N.P., and Clarke, J.D.A., eds., Cool-Water Carbonates: SEPM, Special Publication 56, p. 1–22.

James, N.P., and Bourque, P.-A., 1992, Reefs and mounds, *in* Walker, R.G., and James, N.P., eds., Facies Models: Response to Sea Level Change: St John's, Newfoundland, Geological Association of Canada, p. 323–347.

James, N.P., and von der Borch, C.C., 1991, Carbonate shelf edge off southern Australia: a prograding open platform margin: Geology, v. 19, p. 1005–1008.

James, N.P., Bone, Y., Collins, L.B., and Kyser, T.K., 2001, Surficial sediments of the Great Australian Bight: facies dynamics and oceanography on a vast cool-water carbonate shelf: Journal of Sedimentary Research, v. 71, p. 549–568.

James, N.P., Bone, Y., von der Borch, C.C., and Gostin, V., 1992, Modern carbonate and terrigenous clastic sediments on a cool-water, high-energy, mid-latitude shelf: Lacepede, southern Australia: Sedimentology, v. 39, p. 877–904.

James, N.P., Bone, Y., Hageman, S.J., Feary, D.A., and Gostin, V.A., 1997, Cool-water carbonate sedimentation during the terminal Quaternary sea-level cycle: Lincoln Shelf, southern Australia, *in* James, N.P., and Clarke, J.D.A., eds., Cool-Water Carbonates: SEPM, Special Publication 56, p. 53–76.

James, N.P., Boreen, T.D., Bone, Y., and Feary, D.A., 1994, Holocene carbonate sedimentation on the west Eucla shelf, Great Australian Bight: a shaved shelf: Sedimentology, v. 90, p. 161–178.

James, N.P., Feary, D.A., Surlyk, F., Simo., J.A.T., Betzler, C., Holbourn, A.E., Li, Q., Matsuda, H., Machiyama, H., Brooks, G.R., Andres, M.S., Hine, A.C., and Malone, M.J., 2000, Quaternary bryozoan reef mounds in cool-water, upper slope environments, Great Australian Bight: Geology, v. 26, p. 647–650.

Jennings J.N., 1968, A revised map of the desert dunes of Australia: Australian Geographer, v. 10, p. 408–409.

Li, Q., James, N.P., Bone, Y., and McGowran, B., 1999, Paleoceanographic significance of recent foraminiferal biofacies on the southern shelf of Western Australia: Palaeogeography, Palaeoclimatology, Palaeoecology, v. 147, p. 101–120.

Li, W.-X., Lundberg, J., Dickin, A.P., Ford, D.C., Schwarcz, H.P., and Williams D., 1989, High-precision mass-spectrometric U-series dating of cave deposits and implications for paleoclimate studies: Nature, v. 339, p. 534–536.

Litherland, A.E., and Beukens, R.P., 1995, Radiocarbon dating by atom counting, *in* Rutter, N.W., and Cato, N.R., eds., Dating Methods for Quaternary Deposits: St John's, Newfoundland, Geological Association of Canada, p. 117–123.

Longhurst, A., 1998, Ecological Geography of the Sea: San Diego, California, Academic Press, 398 p.

Lynch-Steiglitz, J., Fairbanks, R.G., and Charles, C.D., 1994, Glacial–interglacial history of Antarctic Intermediate Water: relative strengths of Antarctic versus Indian Ocean waters: Paleoceanography, v. 9, p. 7–29.

Machiyama, H., Yamada, T., Kaneko, N., Iryu, Y., Odawara, R.A., Asami, R., Matsuda, H., Mawatari, S.F., Bone, Y., and James, N.P., 2003, Carbon and oxygen isotopes of cool-water bryozoans from the Great Australian Bight and their paleoenvironmental significance: Proceedings of the Ocean Drilling Program, v. 182, Scientific Results, http://www-odp.tamu/publications/182_SR/007/007_.htm.

Martinson, D.G., Pisias, N.G., Hayes, J.D., Imbrie, J., Moore, T.C., and Shackleton, N.J., 1987, Age dating and the orbital theory of the ice ages: Development of a high-resolution 0 to 300,000-year chronostratigraphy: Quaternary Research, v. 27, p. 1–29.

McKinney, F.K., and Jackson, J.B.C., 1989, Bryozoan Evolution: Boston, Unwin Hyman, 238 p.

Monty, C.L.V., Bosence, D.W.J., Bridges, P.H., and Pratt, B.R., 1995, Carbonate mud-mounds: their origin and evolution: International Association of Sedimentologists, Special Publication 23, 537 p.

Nadeau, M.-J., Schleicher, M., Grootes, P.M., Erlenkeuser, H., Gottdang, A., Mous, D.J.W., Sarnthein, M., and Wilkommen, H., 1997, The Leibniz-Labor AMS facility at the Christian-Albrechts University, Kiel, Germany: Nuclear Instrumentation Methods Physical Research, Section B, v. 123, p. 22–30.

Nelson, C.S., Cooke, P.J., Hendy, C.H., and Cuthbertson, A.M., 1993, Oceanographic and climatic changes over the past 160,000 years at Deep Sea Drilling Project Site 594 off southeastern New Zealand, southwest Pacific Ocean: Paleoceanography, v. 8, p. 435–458.

Okada, H., and Wells, P., 1997, Late Quaternary nannofossil indicators of climate change in two deep-sea cores associated with the Leeuwin Current off Western Australia: Palaeogeography, Palaeoclimatology, Palaeoecology, v. 131, p. 413–432.

Prell, W.L., Hutson, W.H., and Williams, D.F., 1979, The subtropical convergence and late Quaternary circulation in the southern Indian Ocean: Marine Micropaleontology, v. 4, p. 225–234.

Prell, W.L., Hutson, W.H., Williams, D.F., Be, A.W.H., Geitzenauer, K., and Molfino, B., 1980, Surface circulation of the Indian Ocean during the last glacial maximum, approximately 18,000 yr B.P.: Quaternary Research, v. 14, p. 309–336.

Prell, W.L., Imbrie, J., Martinson, D.G., Morley, J.J., Pisias, N.G., Shackleton, N.J., and Streeter, H.F., 1986, Graphic correlation of oxygen isotope stratigraphy application to the late Quaternary: Paleoceanography, v. 1, p. 137–162.

Read, J.F., 1985, Carbonate platform facies models: American Association of Petroleum Geologists, Bulletin, v. 69, p. 1–21.

Schleicher, M., Grootes, P.M., Nadeau, M.-J., and Schoon, A., 1998, The carbonate ^{14}C background and its components at the Leibniz AMS facility: Radiocarbon, v. 40, p. 85–93.

Smith, A.M., and Nelson, C.S., 1996, Differential abrasion of bryozoan skeletons: taphonomic implications for paleoenvironmental interpretation, *in* Gordon, D.P., Smith, A.M., and Grant-

Mackie, J.A., eds., Bryozoans in Space and Time: Wellington, New Zealand, National Institute of Water and Atmospheric Research Ltd., p. 305–313.

SPRIGG, R.C., 1978, Stranded and submerged sea-beach systems of southeast South Australia and the aeolian desert cycle: Sedimentary Geology, v. 22, p. 53–96.

TUCKER, M.E., AND WRIGHT, V.P., 1990, Carbonate Sedimentology: Oxford, U.K., Blackwell Scientific Publications, 482 p.

WASS, R.E., CONNOLLY, J.R., AND MACINTYRE, J., 1970, Bryozoan carbonate sand continuous along southern Australia: Marine Geology, v. 9, p. 63–73.

WELLS, P.E., AND WELLS, G.M., 1994, Large-scale reorganization of ocean currents offshore Western Australia during the late Quaternary: Marine Micropaleontology, v. 24, p. 157–186.

WELLS, P., WELLS, G., CALI, J., AND CHIVAS, A., 1994, Response of deep-sea foraminifera to late Quaternary climate changes, SE Indian Ocean, offshore Western Australia: Marine Micropaleontology, v. 23, p. 185–229.

WILLIAMS, M.A.J., 2001, Quaternary climate changes in Australia and their environmental effects, *in* Gostin, V.A., ed., Gondwana to Greenhouse: Australian Environmental Geoscience, Geological Society of Australia, Special Publication 21, p. 3–11.

WILLIAMS, M., DUNKERLEY, D., DE DECKKER, P., KERSHAW, P., AND CHAPPELL, J., 1998, Quaternary Environments, Second Edition: New York, Oxford University Press, 328 p.

WINSTON, J.E., 1977, Feeding in marine bryozoans, *in* Woollacott, R.M., and Zimmer, R.L., eds., Biology of Bryozoans: New York, Academic Press, p. 233–271.

Received 10 January 2003; accepted 23 June 2003.